Computer Modeling in Engineering & Sciences

Tech Science Press

Doi:10.32604/cmes.2025.067464

ARTICLE

Computational Design of Interval Type-2 Fuzzy Control for Formation and Containment of Multi-Agent Systems with Collision Avoidance Capability

Yann-Horng Lin[1], Wen-Jer Chang[1,*], Yi-Chen Lee[2,*], Muhammad Shamrooz Aslam[3] and Cheung-Chieh Ku[4]

[1]Department of Marine Engineering, National Taiwan Ocean University, Keelung, 202, Taiwan
[2]Department of Information Management, National Sun Yat-Sen University, Kaohsiung, 804, Taiwan
[3]Artificial Intelligence Research Institute, China University of Mining and Technology, Xuzhou, 2211106, China
[4]Department of Marine Engineering, National Kaohsiung University of Science and Technology, Kaohsiung, 811, Taiwan

*Corresponding Authors: Wen-Jer Chang. Email: wjchang@mail.ntou.edu.tw; Yi-Chen Lee. Email: yclee@mis.nsysu.edu.tw

Received: 04 May 2025; Accepted: 01 August 2025; Published: 31 August 2025

ABSTRACT: An Interval Type-2 (IT-2) fuzzy controller design approach is proposed in this research to simultaneously achieve multiple control objectives in Nonlinear Multi-Agent Systems (NMASs), including formation, containment, and collision avoidance. However, inherent nonlinearities and uncertainties present in practical control systems contribute to the challenge of achieving precise control performance. Based on the IT-2 Takagi-Sugeno Fuzzy Model (T-SFM), the fuzzy control approach can offer a more effective solution for NMASs facing uncertainties. Unlike existing control methods for NMASs, the Formation and Containment (F-and-C) control problem with collision avoidance capability under uncertainties based on the IT-2 T-SFM is discussed for the first time. Moreover, an IT-2 fuzzy tracking control approach is proposed to solve the formation task for leaders in NMASs without requiring communication. This control scheme makes the design process of the IT-2 fuzzy Formation Controller (FC) more straightforward and effective. According to the communication interaction protocol, the IT-2 Containment Controller (CC) design approach is proposed for followers to ensure convergence into the region defined by the leaders. Leveraging the IT-2 T-SFM representation, the analysis methods developed for linear Multi-Agent Systems (MASs) are successfully extended to perform containment analysis without requiring the additional assumptions imposed in existing research. Notably, the IT-2 fuzzy tracking controller can also be applied in collision avoidance situations to track the desired trajectories calculated by the avoidance algorithm under the Artificial Potential Field (APF). Benefiting from the combination of vortex and source APFs, the leaders can properly adjust the system dynamics to prevent potential collision risk. Integrating the fuzzy theory and APFs avoidance algorithm, an IT-2 fuzzy controller design approach is proposed to achieve the F-and-C purpose while ensuring collision avoidance capability. Finally, a multi-ship simulation is conducted to validate the feasibility and effectiveness of the designed IT-2 fuzzy controller.

KEYWORDS: Interval type-2 Takagi-Sugeno fuzzy model; multi-agent systems; formation and containment control; fuzzy collision avoidance; artificial potential field

1 Introduction

Prompted by the rapid development of intelligent equipment, control problems under the Multi-Agent System (MAS) framework have proliferated in recent decades [1]. Since the agents can achieve common goals through their own communication, these control issues have become an important milestone for the cooperative control of multiple autonomous vehicles [2]. In various control scenarios, the cooperation of

multiple autonomous devices offers a faster and more efficient solution than using only one device. More importantly, multiple autonomous devices equipped with low-cost onboard systems can serve as a substitute for a single device that relies on high-end equipment [3]. This advantage significantly reduces the cost when the devices require maintenance and are even destroyed. In the broader context of control issues in MASs, cooperative behaviors are primarily discussed in terms of consensus, formation, and containment [4–6]. Consensus control serves as a foundational application for multiple agents to coordinate and reach a common state. Under the leader-follower control framework, consensus means that all follower agents reach the same state as the leader [4]. When there is more than one leader, the consensus problem escalates to the containment problem. Containment control is commonly found in control scenarios where agents with lower capabilities need to be protected by those with higher capabilities and guided into a specific region [5]. Usually, this specific region is defined through the formation control of leaders. Formation control refers to making the agents adhere to a predetermined order to achieve the formation [6]. This feature makes formation control a dominant topic in the research of MASs.

The Formation and Containment (F-and-C) issues have contributed to more efficient achievement of common objectives and broadened the application scope of multi-device control. An increasing number of researchers have also developed composite applications of the Formation Controller (FC) and Containment Controller (CC) using the leader-follower framework [7–9]. However, the safety of agents, especially the leaders, in MASs remains a critical concern due to the dynamic and ever-changing working environments in which autonomous devices operate. Given this consideration, an increasing number of researchers have placed emphasis on the issue of collision avoidance in the control of MASs. Several researchers have also incorporated the collision avoidance mechanism into the design of FC and CC [10,11]. It should be noted that the path planning algorithm plays a crucial role in collision-avoidance methods. Over the past decades, various motion or path planning algorithms have been developed and remained active research topics in collision avoidance scenarios, such as the A* algorithm [12], the dynamic window approach [13], the velocity obstacle method [14], and the Artificial Potential Field (APF) [15]. The collision avoidance mechanisms based on the APF offers advantages such as an intuitive design process, low computational complexity, and reliance on local environmental information. These features make APF particularly suitable for scenarios involving multiple unit encounters and situations requiring rapid emergency responses. For the design of FC and CC, the APF method has also been employed to achieve control objectives while maintaining the capability to avoid collisions between agents [10,11]. Up to now, only a few studies have investigated the collision avoidance issue using the APF in the F-and-C control of MASs.

However, the inherent nonlinearities in system dynamics must be considered due to the complex working environments and the control precision requirements of autonomous devices. With consideration of the interaction protocol, it can be observed that nonlinear dynamic behaviors in Nonlinear MASs (NMASs) significantly complicate the controller design process [4–9]. It is further worth noting that the complexities and challenges are exacerbated when multiple control objectives are required, such as incorporating the collision avoidance issue into F-and-C [10,11]. Solving the control and analysis challenges of systems with nonlinearities, the Takagi-Sugeno Fuzzy Model (T-SFM) has been proposed as an efficient method to convert nonlinear control problems into linear [16–19]. In this manner, nonlinear systems can be linearized into multiple linear subsystems based on a set of fuzzy rules by appropriately selecting premise variables and operating ranges. This characterization enables the design of fuzzy controllers within the linear framework and efficiently reduces the design complexity associated with nonlinear control methods. According to [20], the kinematic components of the mathematical model for the mobile robot exhibit clear nonlinear characteristics. The researchers used the T-SFM to achieve trajectory tracking along with obstacle avoidance capability. Since fuzzy logic and fuzzy inference systems serve as a powerful approach in

decision making, fuzzy theory has gradually been integrated into various obstacle avoidance methods [21,22]. Researchers have also extended the fuzzy-based obstacle avoidance mechanism into the FC design using the APF method [23,24]. However, the collision avoidance using fuzzy logic for the F-and-C control of MASs remains an open issue, especially when considering the integration of APF.

Nevertheless, the so-called type-1 T-SFM used in previous studies [16–20] is insufficient for comprehensively characterizing uncertainties in nonlinear systems. This limitation also results in the corresponding fuzzy controller design methods being unable to handle uncertainties. In widely adopted applications of NMASs, such as unmanned vehicles, uncertainty problem becomes even more critical. These uncertainties may be attributed to discrepancies in the design of membership grades from a linguistic perspective, and structural changes from an application perspective [25,26]. As a result, Type-2 (T-2) fuzzy sets and fuzzy systems have been developed to more comprehensively incorporate uncertain factors into system modeling [27]. A typical T-2 MF consists of primary and secondary membership grades, which results in a three-dimensional structure. However, this structure significantly increases the computational complexity and burden compared to the two-dimensional type-1 MFs [28]. To improve practicality, Interval Type-2 (IT-2) MFs were introduced by setting all secondary membership grades to the maximum value of 1 [29], which reduces computational burden and still maintains a reasonable level of descriptive capability. The IT-2 T-SFM offers better capability for modeling nonlinear systems with uncertainties than type-1 T-SFM, while requiring lower computational resources than the general T-2 T-SFM. Since computational efficiency remains a key concern in real-world control systems, especially in autonomous devices with dynamic uncertainty, this advantage makes IT-2 fuzzy systems a widely adopted solution [30]. Furthermore, due to the close relationship between collision avoidance and decision-making, IT-2 fuzzy logic controllers have been successfully applied to address uncertainties in practical avoidance scenarios [31]. In addition, IT-2 fuzzy control theory provides a powerful framework for NMASs, which involve high computational demands, to mitigate the effects of dynamic uncertainties [32,33].

Although the F-and-C controllers for NMASs have been proposed by some researchers [34,35], the nonlinear frameworks reduce practical applicability and cost-effectiveness. Leveraging the IT-2 T-SFM representation [36], nonlinear control design problems can be recast as the linear problems, while uncertainties are also better handled. As the pioneering work applying IT-2 T-SFM to UNMASs, the researchers in [37] have solved the containment problem of UNMASs under the leader-follower framework. Nevertheless, the leaders are considered as the open-loop systems, which lead to the divergence of the entire UNMAS since the leaders are unstable even though the followers achieve containment. In [38,39], the authors developed the IT-2 fuzzy F-and-C controller design method, which not only guarantees leaders' stability but also achieves the formation objective. In contrast to the existing formation-containment literatures, the design concept of the IT-2 fuzzy FC for leaders is proposed by developing the individual tracking controller. This FC design strategy eliminates the need for communication between the leaders that are farthest apart from each other in the F-and-C problem and enables specifying the entire UNMAS dynamics and time-varying formation without the additional control term in the FC framework. The detailed advantages of the IT-2 F-and-C design method can be found in [39]. However, the safety of agents in UNMASs can only be ensured if the agents possess collision avoidance capabilities. It can be inferred that, since the IT-2 fuzzy F-and-C controller design method for UNMASs was first proposed in [38,39], the collision avoidance issue under this framework has not yet been investigated. Moreover, a novel collision avoidance algorithm is proposed in this research by combining the fuzzy logic and the APF method. Extending the application of fuzzy theory, very few studies have used fuzzy logic to allocate control efforts between modes [40], and research using fuzzy logic to allocate between different APF types remains limited. However, combining different types of APF is a common practice in

collision avoidance. Moreover, these studies on the fuzzy APF method still focus on single control systems. Based on the above statements, the contributions of this research can be summarized as follows:

(1) Building upon the advantages of the IT-2 fuzzy FC design concept in [38,39], an IT-2 fuzzy F-and-C controller design approach combined with a collision avoidance method is first proposed for UNMASs.
(2) A new collision avoidance algorithm is developed by combining the APF method and fuzzy theory, and integrated into the IT-2 fuzzy FC design under the IT-2 T-SFM framework.
(3) Fuzzy logic is used to manage the switching between different APF types, including the vortex APF and the source APF, as well as between the trajectory tracking mode and the collision avoidance mode. In addition, the Distance at Closest Point of Approach (DCPA), commonly applied in avoidance scenarios, is selected to serve as the criterion within the fuzzy logic for determining the switching between modes.

Following the discussion of contributions, the design procedure for this research is presented as follows. First, the IT-2 T-SFM is constructed to more comprehensively represent UNMASs by extending the results in [36]. Leveraging the IT-2 T-SFM and the Imperfect Premise Matching (IPM) concept, the IT-2 fuzzy FC is designed with the tracking control approach, and the IT-2 fuzzy CC is designed with the interaction protocol. Most importantly, the collision avoidance algorithm is proposed by combining fuzzy theory and the APF method into the FC design for the leaders. Since the followers all comply with the dynamics of the leaders, the entire UNMAS can avoid potential collision and obstacle risks if the leaders have the avoidance capability. In this research, a vortex flow serves to steer the agents toward the right-hand side, whereas a source flow serves to repel the agents away from collision points. For the closed-loop IT-2 T-SFM, the IT-2 MF-dependent stability analysis methods are proposed to achieve F-and-C for leaders and followers according to Lyapunov theory. It is worth noting that the desired trajectories calculated by the APF-based method must also be tracked in the avoidance mode, which can efficiently be solved by the IT-2 tracking controller designed for the formation purpose. Finally, the stability conditions are converted into a Linear Matrix Inequality (LMI) problem for the IT-2 fuzzy F-and-C controller design. To verify the feasibility and applicability, a simulation considering multiple ships under the UNMAS structure is conducted.

The organization of this research is as follows. In Section 2, the IT-2 T-SFM and IPM-based fuzzy F-and-C controller are presented for UNMASs. The vortex and source flows are also introduced for the APF method. In Section 3, the stability criteria and IT-2 fuzzy F-and-C controller design with the collision avoidance algorithm are proposed. In Section 4, the simulation results of a multi-ship UNMAS are presented to verify the formation, containment, and collision avoidance performances. In Section 5, some conclusions are presented for the proposed IT-2 fuzzy F-and-C control method.

2 System Description and Problem Statements

In this section, the T-SFM is established for UNMASs based on interval type-2 fuzzy sets. To achieve the tracking objective, an IT-2 T-SFM is also constructed for the target trajectory of UNMASs. By dividing the IT-2 T-SFM into leader and follower models, the IT-2 fuzzy F-and-C controller are respectively developed according to the IPM concept. Subsequently, the definitions of vortex and source flows are introduced to aid the APF-based collision avoidance design. First, the IT-2 T-SFM is presented as follows.

$$\dot{x}_\alpha(t) = \sum_{\ell=1}^{r} \tilde{\Omega}_\ell(v_\alpha(t)) \{\mathbf{A}_\ell x_\alpha(t) + \mathbf{B}_\ell u_\alpha(t)\} \text{ for } \alpha = 1, 2, \ldots, m+n \tag{1}$$

where $x_\alpha(t) \in \mathfrak{R}^s$ and $u_\alpha(t) \in \mathfrak{R}^h$ are the state and input vectors, $v_\alpha(t)$ is the premise variable, $\mathbf{A}_\ell$ and $\mathbf{B}_\ell$ are the constant matrices, ℓ indicates the index of fuzzy rules from 1 to r, α indicates the agent numbers with

the leaders $\alpha = 1, 2, \ldots, m$ and the followers $\alpha = m+1, m+2, \ldots, m+n$. For the IT-2 T-SFM (1), the IT-2 MF $\tilde{\Omega}_\ell(\upsilon_\alpha(t))$ is constructed as follows.

$$\tilde{\Omega}_\ell(\upsilon_\alpha(t)) = \overline{\varepsilon}_\ell(\upsilon_\alpha(t))\,\overline{\Omega}_\ell(\upsilon_\alpha(t)) + \underline{\varepsilon}_\ell(\upsilon_\alpha(t))\,\underline{\Omega}_\ell(\upsilon_\alpha(t)) \tag{2}$$

where $\sum_{\ell=1}^{r} \tilde{\Omega}_\ell(\upsilon_\alpha(t)) = 1$, $\overline{\Omega}_\ell(\upsilon_\alpha(t)) = \prod_{q=1}^{z} \overline{\omega}_{\ell q}(\upsilon_{\alpha q}(t)) \geq 0$ and $\underline{\Omega}_\ell(\upsilon_\alpha(t)) = \prod_{q=1}^{z} \underline{\omega}_{\ell q}(\upsilon_{\alpha q}(t)) \geq 0$ are the upper bound and lower bound grades of membership which satisfy the relationship $1 \geq \overline{\Omega}_\ell(\upsilon_\alpha(t)) \geq \underline{\Omega}_\ell(\upsilon_\alpha(t)) \geq 0$, $\overline{\omega}_{\ell q}(\upsilon_{\alpha q}(t))$ and $\underline{\omega}_{\ell q}(\upsilon_{\alpha q}(t))$ are the upper and lower bound MFs inferred from If-Then fuzzy rules, which satisfy the relationship $1 \geq \overline{\omega}_{\ell q}(\upsilon_{\alpha q}(t)) \geq \underline{\omega}_{\ell q}(\upsilon_{\alpha q}(t)) \geq 0$, q indicates the index of premise variables from 1 to z. Note that $\overline{\varepsilon}_\ell(\upsilon_\alpha(t))$ and $\underline{\varepsilon}_\ell(\upsilon_\alpha(t))$ in (2) are nonlinear functions associated with the uncertain factors and are not required to be known. These functions also satisfy the relationship $1 \geq \overline{\varepsilon}_\ell(\upsilon_\alpha(t)) \geq \underline{\varepsilon}_\ell(\upsilon_\alpha(t)) \geq 0$ and $\overline{\varepsilon}_\ell(\upsilon_\alpha(t)) + \underline{\varepsilon}_\ell(\upsilon_\alpha(t)) = 1$. The detailed modeling information of the IT-2 T-SFM can be found in [36].

For the formation of leaders under the tracking control framework, the IT-2 T-SFM of the target trajectory is constructed in a similar manner to (1).

$$\dot{x}_\alpha^d(t) = \sum_{\ell=1}^{r} \tilde{\Omega}_\ell(\upsilon_\alpha(t)) \left\{ \mathbf{A}_\ell x_\alpha^d(t) \right\} \text{ for } \alpha = 1, 2, \ldots, m \tag{3}$$

For the followers in UNMASs, the interaction protocol is considered through communication between agents to achieve the containment purpose. Because of this reason, the definition of the interaction relationship for the followers in IT-2 T-SFM (1) is provided based on graph theory as follows.

Definition 1: *For an undirected graph $\mathbb{G} = (M, C, \mathcal{A})$, the node set is defined for all the nodes as $M = \{\mu_1, \mu_2, \ldots, \mu_{m+n}\}$, and the edge set is defined as $C \subseteq M \times M$. Thus, $(\mu_\alpha, \mu_\gamma) \in C$ indicates the existence of an edge between nodes μ_α and μ_γ. For the neighbor nodes of node μ_α, the corresponding set is defined as $N = \{\mu_\gamma \in M : (\mu_\alpha, \mu_\gamma) \in C\}$. Based on the definitions of M, C and N, the adjacency matrix is formulated as $\mathcal{A} = [a_{\alpha\gamma}] \in \Re^{(m+n)\times(m+n)}$ to represent the relationships among all nodes, in which the elements $a_{\alpha\gamma}$ with the values 1 and 0 respectively indicate $(\mu_\alpha, \mu_\gamma) \in C$ and $(\mu_\alpha, \mu_\gamma) \notin C$. Then, the degree matrix $\mathcal{D} = [d_{\alpha\alpha}] \in \Re^{(m+n)\times(m+n)}$ is also formulated by these elements with the calculation $d_{\alpha\alpha} = \sum_{\gamma=1}^{m+n} a_{\alpha\gamma}$ where $\alpha \neq \gamma$. By subtracting the adjacent matrix from degree matrix, the so-called Laplacian matrix is obtained as $\mathbf{L} = \mathcal{D} - \mathcal{A}$.*

Based on Definition 1, the agents in UNMASs are denoted as nodes while the interaction relationships are denoted as edges. In most leader-follower structures, the leaders serve as units to detect environmental changes and potential dangers, subsequently commanding the followers for control purposes. That is to say, the leaders do not acquire information from other agents. As a result, the Laplacian matrix $\mathbf{L}$ is further divided into the following form.

$$\mathbf{L} = \begin{bmatrix} \mathbf{0}_{m\times m} & \mathbf{0}_{m\times n} \\ \mathbf{L}_2 & \mathbf{L}_1 \end{bmatrix} \tag{4}$$

where $\mathbf{L}_1$ and $\mathbf{L}_2$ represent the interactions between followers and from leaders to followers, respectively. Note that the Laplacian matrix in (4) is widely used to incorporate interaction relationship into the control design of leader-follower MASs.

Referring to [37], the properties of the Laplacian matrix (4) are presented in Lemma 1.

Lemma 1 [37]**:** *All eigenvalues of matrix* $\mathbf{L}_1$ *have positive real parts. The nonnegative matrix* $-\mathbf{L}_1^{-1}\mathbf{L}_2$ *has the property that the sum of each row equals one.*

In this research, it is assumed that there is at least one interaction from each leader to the followers. Then, dividing the IT2 T-SFM (1) into the leader and follower parts, the following tracking error model for the leader is obtained by subtracting (3) from the leader's T-SFM.

$$\dot{e}_\alpha(t) = \sum_{\ell=1}^{r} \tilde{\Omega}_\ell(v_\alpha(t)) \{\mathbf{A}_\ell e_\alpha(t) + \mathbf{B}_\ell u_\alpha(t)\} \text{ for } \alpha = 1, 2, \ldots, m \tag{5}$$

where $e_\alpha(t) = x_\alpha(t) - x_\alpha^d(t)$ represents the tracking error of system states.

Therefore, the tracking objective can be achieved by designing the control input $u_\alpha(t)$ to ensure the stability of the error model (5) for each leader. This implies that the leaders' dynamics will converge to the desired target dynamics. By appropriately assigning different target dynamics to each leader, the formation objective can thus be accomplished.

For the error model (5) of leaders and the followers in the IT-2 T-SFM (1), the IT-2 fuzzy controller is designed as follows to achieve the F-and-C objectives.

$$u_\alpha(t) = \sum_{\tau=1}^{v} \tilde{\Psi}_\tau(v_\alpha(t)) \{\mathbf{F}_\tau e_\alpha(t)\} \text{ for } \alpha = 1, 2, \ldots, m \tag{6}$$

$$u_\alpha(t) = \sum_{\tau=1}^{v} \tilde{\Psi}_\tau(v_\alpha(t)) \left\{\mathbf{K}_\tau \sum_{\gamma \in N} a_{\alpha\gamma}\left(x_\alpha(t) - x_\gamma(t)\right)\right\} \text{ for } \alpha = m+1, m+2, \ldots, m+n \tag{7}$$

where $\mathbf{F}_\tau$ and $\mathbf{K}_\tau$ are the control gains for the F-and-C objectives, $\tilde{\Psi}_\tau(v_\alpha(t))$ is the IT-2 MF of fuzzy controller derived as follows.

$$\tilde{\Psi}_\tau(v_\alpha(t)) = \frac{\overline{\vartheta}_\tau(v_\alpha(t))\,\overline{\Psi}_\tau(v_\alpha(t)) + \underline{\vartheta}_\tau(v_\alpha(t))\,\underline{\Psi}_\tau(v_\alpha(t))}{\sum_{o=1}^{v}\left(\overline{\vartheta}_o(v_\alpha(t))\,\overline{\Psi}_o(v_\alpha(t)) + \underline{\vartheta}_o(v_\alpha(t))\,\underline{\Psi}_o(v_\alpha(t))\right)} \tag{8}$$

where $\sum_{\tau=1}^{v} \tilde{\Psi}_\tau(v_\alpha(t)) = 1$, $\overline{\Psi}_\tau(v_\alpha(t)) = \prod_{q=1}^{z} \overline{\psi}_{\tau q}\left(v_{\alpha q}(t)\right) \geq 0$ and $\underline{\Psi}_\tau(v_\alpha(t)) = \prod_{q=1}^{z} \underline{\psi}_{\tau q}\left(v_{\alpha q}(t)\right) \geq 0$ are the upper bound and lower bound grades of membership, $\overline{\psi}_{\tau q}\left(v_{\alpha q}(t)\right)$ and $\underline{\psi}_{\tau q}\left(v_{\alpha q}(t)\right)$ are the upper and lower bound MFs. Note that these membership grades and MFs satisfy the same condition as those in IT-2 T-SFM (1). Different from the IT-2 T-SFM, $\overline{\vartheta}_\tau(v_\alpha(t))$ and $\underline{\vartheta}_\tau(v_\alpha(t))$ are the predefined functions since the fuzzy controller is developed by the designers.

It is worth noting that the MFs as well as the fuzzy rules of FC and CC in (6) and (7) can be designed differently due to the IPM concept. This feature makes the fuzzy controller design process more flexible and helps reduce application complexity by using fewer rules in the controller. Accordingly, the closed-loop error model for leaders can be obtained by substituting (6) into (5) as follows.

$$\dot{e}_\alpha(t) = \sum_{\ell=1}^{r} \sum_{\tau=1}^{v} \tilde{\Omega}_\ell(v_\alpha(t))\,\tilde{\Psi}_\tau(v_\alpha(t)) \{(\mathbf{A}_\ell + \mathbf{B}_\ell \mathbf{F}_\tau) e_\alpha(t)\} \text{ for } \alpha = 1, 2, \ldots, m \tag{9}$$

From (9), it can be observed that if the tracking error converges through the design of gain $\mathbf{F}_\rho$, the formation objective can be achieved by assigning different target trajectories to different leaders. This formation control strategy eliminates the need for communication between leaders and effectively mitigates

faults arising from signal transmission. Obviously, leaders are the most critical components in UNMASs, and the enhancement of safety has therefore become a crucial issue.

To achieve the containment objective for followers, the closed-loop IT-2 T-SFM is obtained as follows by substituting (7) into (1).

$$\dot{x}_F(t) = \sum_{\ell=1}^{r}\sum_{\tau=1}^{v} \tilde{\Omega}_\ell(v_F(t))\,\tilde{\Psi}_\tau(v_F(t))\left\{\left(\mathbf{I}_n \otimes \mathbf{A}_\ell + \mathbf{L}_1 \otimes \mathbf{B}_\ell \mathbf{K}_\tau\right) x_F(t) + \left(\mathbf{L}_2 \otimes \mathbf{B}_\ell \mathbf{K}_\tau\right) x_L(t)\right\} \tag{10}$$

where $\mathbf{I}$ is the identity matrix with a dimension determined by the number of followers, $\otimes$ is the Kronecker product, the state vectors are $x_F(t) = \begin{bmatrix} x_{m+1}(t) & x_{m+2}(t) & \cdots & x_{m+n}(t) \end{bmatrix}^{\mathrm{T}} \in \Re^{(s\times n)}$ and $x_L(t) = \begin{bmatrix} x_1(t) & x_2(t) & \cdots & x_m(t) \end{bmatrix}^{\mathrm{T}} \in \Re^{(s\times m)}$.

Nevertheless, the analysis process for fuzzy CC design may become increasingly conservative as both the number of agents and the fuzzy rules escalate due to the growing number of stability conditions. To solve the problem, an analysis approach for the containment analysis of the IT-2 T-SFM (10) as follows.

Lemma 2 [41]: *Let λ_α denote the eigenvalues and $J_{\mathbf{L}_1} = \mathbf{W}^{-1}\mathbf{L}_1\mathbf{W}$ denote the Jordan canonical form of the matrix $\mathbf{L}_1$, where $\mathbf{W}$ is a nonsingular matrix. The eigenvalues are reordered following the relationship $Re\{\lambda_{m+1}\} < Re\{\lambda_{m+2}\} < \ldots < Re\{\lambda_{m+n}\}$ in which $Re\{\bullet\}$ denotes the real part of $\cdot$. Thus, the following result is obtained.*

$$\begin{aligned} &If\ the\ condition\ \boldsymbol{\Theta}_1 + Re\left\{\tilde{\lambda}_\beta\right\}\boldsymbol{\Theta}_2 + Im\left\{\tilde{\lambda}_\beta\right\}\boldsymbol{\Theta}_3 < 0 \quad for \quad \beta = 1,2,3,4 \quad is\ satisfied,\\ &then\ the\ \boldsymbol{\Theta}_1 + Re\left\{\lambda_\alpha\right\}\boldsymbol{\Theta}_2 + Im\left\{\lambda_\alpha\right\}\boldsymbol{\Theta}_3 < 0 \quad for\ \alpha = m+1, m+2, \ldots, m+n\ is\ also\ satisfied. \end{aligned} \tag{11}$$

where $\tilde{\lambda}_{1,2} = Re\{\lambda_{m+1}\} \pm jmax\{Im\{\lambda_\alpha\}\}$ and $\tilde{\lambda}_{3,4} = Re\{\lambda_{m+n}\} \pm jmax\{Im\{\lambda_\alpha\}\}$, $Im\{\bullet\}$ denotes the imaginary part of $\cdot$, $\boldsymbol{\Theta}_1$, $\boldsymbol{\Theta}_2$ and $\boldsymbol{\Theta}_3$ are the real symmetric matrices.

Owing to the representation of IT-2 T-SFM, Lemma 2 can be utilized for the followers in UNMASs. From Lemma 2, it can be seen that the conditions in (11) are presented in LMI form. Moreover, the condition (11) indicates that only four LMI conditions need to be solved during the containment analysis process, regardless of how many followers are present in the UNMASs. This reduction in the number of stability conditions significantly benefits the controller design method based on the T-SFM, since the number of conditions tends to increase with the number of rules.

After the F-and-C objectives are ensured for leaders and followers, the collision avoidance requirement must also be considered for the safety improvement of UNMASs. By combining the fuzzy theory with the APF method, the collision avoidance algorithm is incorporated into the IT-2 fuzzy F-and-C controller design process. However, one of the most critical issues in the APF method is the deadlock problem. Based on the results in [42], a velocity potential field design approach is presented to efficiently avoid deadlock in collision avoidance situations.

Remark 1: *Referring to [42], no deadlock exists within the region if the velocity potential function Φ is a harmonic function and continuous throughout the entire region.*

Since the prerequisite information required by the APF method is difficult to be directly provided based on the state vector of the IT-2 T-SFM (9) and (10), the states of the leader agents are preliminarily assumed as follows for the application. Specifically, the X and Y positions, yaw angle on the earth-fixed frame, as well as the longitudinal and lateral velocities and yaw angular velocity on the body-fixed frame, are typically considered in trajectory tracking problems. Therefore, the states are set as $(x_{\alpha 1}(t), x_{\alpha 2}(t)) = (X_\alpha(t), Y_\alpha(t))$ and $(x_{\alpha 4}(t), x_{\alpha 5}(t)) = \left(V_{x\alpha}(t), V_{y\alpha}(t)\right)$ for $\alpha = 1,2,\ldots,m$ in the theoretical part, which

can also be seen in the simulation section. Considering Remark 1, the velocity potential functions of vortex and source flows are respectively introduced as follows for the application of APF method.

Definition 2: *The vortex potential field and the corresponding gradient are given as follows.*

$$\Phi_{v\sigma} = k_v\theta_\sigma \text{ and } \nabla\Phi_{v\sigma} = \left(v_{vx\sigma}, v_{vy\sigma}\right) = \left(-k_v\left(\frac{x_{\alpha 2}(t) - y_\sigma^c(t)}{R_\sigma}\right), k_v\left(\frac{x_{\alpha 1}(t) - x_\sigma^c(t)}{R_\sigma}\right)\right) \tag{12}$$

Definition 3: *The source potential field and the corresponding gradient are given as follows.*

$$\Phi_{s\sigma} = k_s \ln\left(R_\sigma\right) \text{ and } \nabla\Phi_{s\sigma} = \left(v_{sx\sigma}, v_{sy\sigma}\right) = \left(\frac{k_s}{R_\sigma} cos\left(\theta_\sigma\right), \frac{k_s}{R_\sigma} sin\left(\theta_\sigma\right)\right) \tag{13}$$

where $R_\sigma = \sqrt{\left(x_{\alpha 1}(t) - x_\sigma^c(t)\right)^2 + \left(x_{\alpha 2}(t) - y_\sigma^c(t)\right)^2}$, $\theta_\sigma = atan2\left(\frac{x_{\alpha 2}(t) - y_\sigma^c(t)}{x_{\alpha 1}(t) - x_\sigma^c(t)}\right)$, $x_\sigma^c(t)$ *and* $y_\sigma^c(t)$ *are the X and Y positions of collisions to be avoided, the index* σ *denotes the* σ-th *collision,* v_r *is the radial velocity and* v_θ *is the tangential velocity,* k_v *and* k_s *are respectively the intensities of vortex and source flows, the symbol* ∇ *denotes the gradient operator.*

Note that the vortex potential field is defined with a counterclockwise direction to adjust the agents toward the right-hand side in this research. Moreover, the source potential field serves as an APF to repulse the agents away from the collision events. According to the theory of APF method, it is known that if only the source APF is applied in the collision avoidance mechanism, the agent may become stuck at a point in front of the obstacle when the target is located directly behind the obstacle. In addition, if only the vortex APF is applied, the agent may keep circling around the obstacle without reaching the target. Based on the definitions in (12) and (13), these undesired behaviors become more significant as the agent gets closer to the obstacle, which corresponds to the center of the APFs. To overcome these problems, a combined application of the source APF and the vortex APF is proposed in this research through the use of fuzzy logic. The key function of fuzzy logic is that the abrupt changes caused by the switching between different APFs can be reduced, and smoother avoidance behavior can be realized.

In addition to the APF method, the Time to Closest Point of Approach (TCPA) and Distance at Closest Point of Approach (DCPA) are commonly used for the assessment of collision situations and risks. The concepts of TCPA and DCPA have been widely applied in collision avoidance for autonomous vehicles. Incorporating these factors into the development of collision avoidance algorithms enables agents to achieve more precise avoidance performance. Based on the above setting for the system states, the TCPA and DCPA are presented in Definition 4.

Definition 4: *The TCPA and DCPA for all potential collisions are defined using the positions* $x_{\alpha 1}(t)$, $x_{\alpha 2}(t)$ *and velocities* $x_{\alpha 4}(t)$, $x_{\alpha 5}(t)$ *as follows.*

$TCPA_\sigma$:

$$-\frac{\tilde{R}_\sigma \cdot \tilde{V}_\sigma}{\left|\tilde{V}_\sigma\right|^2} = -\frac{\left(x_\sigma^c(t) - x_{\alpha 1}(t)\right)\left(V_{x\sigma}^c(t) - x_{\alpha 4}(t)\right) + \left(y_\sigma^c(t) - x_{\alpha 2}(t)\right)\left(V_{y\sigma}^c(t) - x_{\alpha 5}(t)\right)}{\left(V_{x\sigma}^c(t) - x_{\alpha 4}(t)\right)^2 + \left(V_{y\sigma}^c(t) - x_{\alpha 5}(t)\right)^2} \tag{14}$$

$DCPA_\sigma$:

$$\begin{aligned}&\left|\tilde{R}_\sigma + \text{TCPA}_\sigma \cdot \tilde{V}_\sigma\right| \\ &= \sqrt{\left(x_\sigma^c(t) - x_{\alpha 1}(t) + \text{TCPA}_\sigma\left(V_{x\sigma}^c(t) - x_{\alpha 4}(t)\right)\right)^2 + \left(y_\sigma^c(t) - x_{\alpha 2}(t) + \text{TCPA}_\sigma\left(V_{y\sigma}^c(t) - x_{\alpha 5}(t)\right)\right)^2}\end{aligned} \tag{15}$$

where the vectors $\tilde{R}_\sigma = \left(x_\sigma^c(t) - x_{\alpha 1}(t), y_\sigma^c(t) - x_{\alpha 2}(t)\right)$ *and* $\tilde{V}_\sigma = \left(V_{x\sigma}^c(t) - x_{\alpha 4}(t), V_{y\sigma}^c(t) - x_{\alpha 5}(t)\right)$ *are the relative positions and velocities.*

Within the collision avoidance framework, the TCPA and DCPA parameters are utilized to assess whether a potential collision event is imminent within the detection range. Specifically, when the conditions based on TCPA and DCPA are satisfied, the leaders transition into collision avoidance mode; otherwise, the leaders maintain tracking mode. Upon entering collision avoidance mode, the target trajectories used in the IT-2 fuzzy formation controller (6) are generated by combining the vortex APF in Definition 2 and the source APF in Definition 3. Moreover, fuzzy logic is applied in this research to achieve smoother adjustment between the two APFs.

Therefore, an IT-2 fuzzy F-and-C controller design approach combined with the collision avoidance algorithm is proposed for UNMASs based on the IT-2 T-SFMs (9) and (10) and the APF method from Definitions 2–4. Moreover, Lemma 2 is also applied to obtain a more relaxed containment analysis process for followers.

3 Interval Type-2 Fuzzy Controller Design for Multiple Objectives

According to the IT-2 T-SFM (9) of tracking error, a more convenient stability criterion is proposed to achieve FC design objectives in this section. By virtue of this design scheme, a collision avoidance algorithm combining the APF method with fuzzy theory is also proposed for the leaders in UNMASs. After the collision-free formation controller has been designed, the IT-2 fuzzy CC design approach can be proposed for followers based on the interaction relationship among all agents. Therefore, the entire UNMAS can avoid potential collisions through the IT-2 fuzzy FC design and the control commands of leaders. Since the followers are ensured to converge into the leaders' formation, their safety is certainly guaranteed by IT-2 fuzzy CC. First, a stability criterion for the IT-2 fuzzy FC design is proposed as follows based on the Lyapunov theory and the IPM concept.

Theorem 1: *If there exist the positive definite matrices* $\mathbf{Q}^L$, $\mathbf{H}_{\ell\tau}^L$, *the symmetric matrix* $\mathbf{S}^L$ *and the matrices* $\mathbf{G}_\tau$ *such that the following conditions are all satisfied based on the given scalars* $\overline{\eta}_{\ell\tau i_1 i_2 \cdots i_z \kappa}^L$ *and* $\underline{\eta}_{\ell\tau i_1 i_2 \cdots i_z \kappa}^L$, *the error dynamic in the IT-2 T-SFM (9) is asymptotically stable.*

$$\mathbf{Q}^L > 0 \text{ and } \mathbf{H}_{\ell\tau}^L > 0 \tag{16}$$

$$\mathbf{A}_\ell \mathbf{Q}^L + \mathbf{Q}^L \mathbf{A}_\ell^{\mathrm{T}} + \mathbf{B}_\ell \mathbf{G}_\tau + \mathbf{G}_\tau^{\mathrm{T}} \mathbf{B}_\ell^{\mathrm{T}} - \mathbf{H}_{\ell\tau}^L + \mathbf{S}^L < 0 \text{ for } \ell = 1, .., r, \tau = 1, .., \nu \tag{17}$$

$$\sum_{\ell=1}^{r} \sum_{\tau=1}^{\nu} \left(\underline{\eta}_{\ell\tau i_1 i_2 \cdots i_z \kappa}^L \left(\mathbf{A}_\ell \mathbf{Q}^L + \mathbf{Q}^L \mathbf{A}_\ell^{\mathrm{T}} + \mathbf{B}_\ell \mathbf{G}_\tau + \mathbf{G}_\tau^{\mathrm{T}} \mathbf{B}_\ell^{\mathrm{T}} \right) - \left(\underline{\eta}_{\ell\tau i_1 i_2 \cdots i_z \kappa}^L - \overline{\eta}_{\ell\tau i_1 i_2 \cdots i_z \kappa}^L \right) \mathbf{H}_{\ell\tau}^L + \underline{\eta}_{\ell\tau i_1 i_2 \cdots i_z \kappa}^L \mathbf{S}^L \right) - \mathbf{S}^L < 0$$

$$\text{for } i_1, i_2 \cdots i_z = 1, 2, \ \kappa = 1, 2, \ldots, \delta^L \tag{18}$$

where $\mathbf{G}_\tau = \mathbf{F}_\tau \mathbf{Q}^L$ *and* $\mathbf{Q}^L = \mathbf{P}_L^{-1}$, $\overline{\eta}_{\ell\tau i_1 i_2 \cdots i_z \kappa}^L$ *and* $\underline{\eta}_{\ell\tau i_1 i_2 \cdots i_z \kappa}^L$ *are the IT-2 MF-dependent parameters, in which* i_1 *to* i_z *are the parameters associated with the number of premise variables, and* κ *denotes the division of the sub-state space in the MF-dependent analysis method. The detailed definition and information of these parameters will be provided later in the derivation.*

Proof of Theorem 1: In this research, the formation control objective is achieved through individual trajectory tracking controllers for each leader. That is, due to the homogeneity among UNMASs, the stability analysis is only required to be developed for one leader. Accordingly, the Lyapunov function is defined as follows for the stability analysis.

$$V_L\left(e_1(t)\right) = e_1^{\mathrm{T}}(t) \mathbf{P}_L e_1(t) \tag{19}$$

where $\mathbf{P}_L$ is the positive definite matrix. Then, the following derivative is obtained from (19).

$$\dot{V}_L\left(e_1\left(t\right)\right)=\sum_{\ell=1}^{r}\sum_{\tau=1}^{v}\tilde{\Omega}_\ell\left(v_1\left(t\right)\right)\tilde{\Psi}_\tau\left(v_1\left(t\right)\right)\left\{e_1^{\mathrm{T}}\left(t\right)\left(\mathbf{A}_\ell^{\mathrm{T}}\mathbf{P}_L+\mathbf{P}_L\mathbf{A}_\ell+\mathbf{F}_\tau^{\mathrm{T}}\mathbf{B}_\ell^{\mathrm{T}}\mathbf{P}_L+\mathbf{P}_L\mathbf{B}_\ell\mathbf{F}_\tau\right)e_1\left(t\right)\right\} \tag{20}$$

It is known that the Lyapunov function (19) is defined for the tracking errors from an energy perspective. That is, if the derivative (20) of the Lyapunov function, which denotes the rate of energy change, is ensured to be negative, then the energy of the tracking error dynamics will converge to zero. This also implies that the leader dynamics can approach the desired target dynamics.

To simplify the IT-2 MF-dependent analysis method, $\tilde{\Gamma}_{\ell\tau}\left(v_1\left(t\right)\right)=\tilde{\Omega}_\ell\left(v_1\left(t\right)\right)\tilde{\Psi}_\tau\left(v_1\left(t\right)\right)$ is adopted to define the MF throughout the rest of the research. Usually, the analysis process of the type-1 T-SFM involves making the matrix within the error vector in (20) negative definite. However, this approach is too conservative for the IT-2 T-SFM that a more detailed discussion can be found in [36]. Because of this reason, the IT-2 MF-dependent analysis method is presented as follows. First, the MF is represented in the following form.

$$\tilde{\Gamma}_{\ell\tau}\left(v_1\left(t\right)\right)=\overline{\omega}_{\ell\tau}\left(v_1\left(t\right)\right)\overline{\Gamma}_{\ell\tau}\left(v_1\left(t\right)\right)+\underline{\omega}_{\ell\tau}\left(v_1\left(t\right)\right)\underline{\Gamma}_{\ell\tau}\left(v_1\left(t\right)\right) \tag{21}$$

where $\overline{\omega}_{\ell\tau}\left(v_1\left(t\right)\right)$ and $\underline{\omega}_{\ell\tau}\left(v_1\left(t\right)\right)$ are functions that also do not need to be known because of $\overline{\varepsilon}_\ell\left(v_1\left(t\right)\right)$ and $\underline{\varepsilon}_\ell\left(v_1\left(t\right)\right)$, and the relationship $1\geq\overline{\omega}_{\ell\tau}\left(v_1\left(t\right)\right)\geq\underline{\omega}_{\ell\tau}\left(v_1\left(t\right)\right)\geq 0$ is also satisfied.

Subsequently, the upper and lower bound MFs in (21) can be defined as follows.

$$\overline{\Gamma}_{\ell\tau}\left(v_1\left(t\right)\right)=\sum_{\kappa=1}^{\delta}\sum_{i_1=1}^{2}\cdots\sum_{i_z=1}^{2}\prod_{q=1}^{z}\chi_{qi_q\kappa}\left(v_q^1\left(t\right)\right)\overline{\eta}_{\ell\tau i_1 i_2\cdots i_z\kappa}^{L} \tag{22}$$

$$\underline{\Gamma}_{\ell\tau}\left(v_1\left(t\right)\right)=\sum_{\kappa=1}^{\delta}\sum_{i_1=1}^{2}\cdots\sum_{i_z=1}^{2}\prod_{q=1}^{z}\chi_{qi_q\kappa}\left(v_q^1\left(t\right)\right)\underline{\eta}_{\ell\tau i_1 i_2\cdots i_z\kappa}^{L} \tag{23}$$

where $\chi_{qi_q\kappa}\left(v_q^1\left(t\right)\right)$ is the so-called cross term for both upper and lower bound MFs satisfying the conditions $1\geq\chi_{qi_q\kappa}\left(v_q^1\left(t\right)\right)\geq 0$ and $\chi_{q1\kappa}\left(v_q^1\left(t\right)\right)+\chi_{q2\kappa}\left(v_q^1\left(t\right)\right)=1$ for all i_q, and the parameters satisfy the condition $1\geq\overline{\eta}_{\ell\tau i_1 i_2\cdots i_z\kappa}^{L}\geq\underline{\eta}_{\ell\tau i_1 i_2\cdots i_z\kappa}^{L}\geq 0$.

Then, the parameter κ is given from the δ^L connected sub-state space denoted as M_κ in the state space of interest, $\mathrm{M}=\cup_{\kappa=1}^{\delta^L}\mathrm{M}_\kappa$. The detailed process of constructing the parameters in (21)–(23) can be found in (25)–(28) and Remarks 5 and 6 of [36]. Based on the definition of (21), the derivative of Lyapunov function can be derived as follows by multiplying $\mathbf{P}_L^{-1}$ on the right and left-hand sides.

$$\begin{aligned}\dot{V}_L\left(e_1\left(t\right)\right)=&\sum_{\ell=1}^{r}\sum_{\tau=1}^{v}\left(\overline{\omega}_{\ell\tau}\left(v_1\left(t\right)\right)\overline{\Gamma}_{\ell\tau}\left(v_1\left(t\right)\right)+\underline{\omega}_{\ell\tau}\left(v_1\left(t\right)\right)\underline{\Gamma}_{\ell\tau}\left(v_1\left(t\right)\right)\right)\\&\times\left\{e_1^{\mathrm{T}}\left(t\right)\left(\mathbf{Q}^L\mathbf{A}_\ell^{\mathrm{T}}+\mathbf{A}_\ell\mathbf{Q}^L+\mathbf{G}_\tau^{\mathrm{T}}\mathbf{B}_\ell^{\mathrm{T}}+\mathbf{B}_\ell\mathbf{G}_\tau\right)e_1\left(t\right)\right\}\end{aligned} \tag{24}$$

In relation to the IT-2 MFs, the slack matrices are introduced as follows.

$$\left(\sum_{\ell=1}^{r}\sum_{\tau=1}^{v}\left(\overline{\omega}_{\ell\tau}\left(v_1\left(t\right)\right)\overline{\Gamma}_{\ell\tau}\left(v_1\left(t\right)\right)+\underline{\omega}_{\ell\tau}\left(v_1\left(t\right)\right)\underline{\Gamma}_{\ell\tau}\left(v_1\left(t\right)\right)\right)-1\right)\mathbf{S}^L=0 \tag{25}$$

$$-\sum_{\ell=1}^{r}\sum_{\tau=1}^{v}\left(1-\overline{\omega}_{\ell\tau}\left(v_1\left(t\right)\right)\right)\left(\underline{\Gamma}_{\ell\tau}\left(v_1\left(t\right)\right)-\overline{\Gamma}_{\ell\tau}\left(v_1\left(t\right)\right)\right)\mathbf{H}_{\ell\tau}^{L}\geq 0 \tag{26}$$

Based on the properties of the IT-2 MFs, it can be readily verified that equality (25) and inequality (26) hold. These slack matrices are combined into the stability analysis and stability conditions as additional variables to be solved using LMI techniques. It is known that increasing the number of variables in the stability conditions can reduce conservatism when solving the control problem under stability criteria. With the combination of (25) and (26), the relationship for (24) is derived as follows.

$$\begin{aligned}\dot{V}_L\left(e_1(t)\right) \leq e_1^{\mathrm{T}}(t)\Bigg(&\sum_{\ell=1}^{r}\sum_{\tau=1}^{v}\left(\underline{\Gamma}_{\ell\tau}\left(v_1(t)\right)\left(\mathbf{Q}^L\mathbf{A}_\ell^{\mathrm{T}}+\mathbf{A}_\ell\mathbf{Q}^L+\mathbf{G}_\tau^{\mathrm{T}}\mathbf{B}_\ell^{\mathrm{T}}+\mathbf{B}_\ell\mathbf{G}_\tau\right)\right.\\&\left.-\left(\underline{\Gamma}_{\ell\tau}\left(v_1(t)\right)-\overline{\Gamma}_{\ell\tau}\left(v_1(t)\right)\right)\mathbf{H}_{\ell\tau}^L+\underline{\Gamma}_{\ell\tau}\left(v_1(t)\right)\mathbf{S}^L\right)-\mathbf{S}^L\Bigg)e_1(t)\\&-\sum_{\ell=1}^{r}\sum_{\tau=1}^{v}\left(\overline{\omega}_{\ell\tau}\left(v_1(t)\right)\left(\underline{\Gamma}_{\ell\tau}\left(v_1(t)\right)-\overline{\Gamma}_{\ell\tau}\left(v_1(t)\right)\right)\right.\\&\left.\times e_1^{\mathrm{T}}(t)\left(\mathbf{Q}^L\mathbf{A}_\ell^{\mathrm{T}}+\mathbf{A}_\ell\mathbf{Q}^L+\mathbf{G}_\tau^{\mathrm{T}}\mathbf{B}_\ell^{\mathrm{T}}+\mathbf{B}_\ell\mathbf{G}_\tau-\mathbf{H}_{\ell\tau}^L+\mathbf{S}^L\right)e_1(t)\right)\end{aligned}\tag{27}$$

Consequently, the following results can be obtained by extracting the cross term from the right-hand side of inequality (27).

$$\begin{aligned}&e_1^{\mathrm{T}}(t)\Bigg(\chi_{qi_q\kappa}\left(v_q^1(t)\right)\sum_{\ell=1}^{r}\sum_{\tau=1}^{v}\left(\underline{\eta}_{\ell\tau i_1 i_2\cdots i_z\kappa}^L\left(\mathbf{Q}^L\mathbf{A}_\ell^{\mathrm{T}}+\mathbf{A}_\ell\mathbf{Q}^L+\mathbf{G}_\tau^{\mathrm{T}}\mathbf{B}_\ell^{\mathrm{T}}+\mathbf{B}_\ell\mathbf{G}_\tau\right)\right.\\&\left.-\left(\underline{\eta}_{\ell\tau i_1 i_2\cdots i_z\kappa}^L-\overline{\eta}_{\ell\tau i_1 i_2\cdots i_z\kappa}^L\right)\mathbf{H}_{\ell\tau}^L+\underline{\eta}_{\ell\tau i_1 i_2\cdots i_z\kappa}^L\mathbf{S}^L\right)-\mathbf{S}^L\Bigg)e_1(t)\\&-\chi_{qi_q\kappa}\left(v_q^1(t)\right)\sum_{\ell=1}^{r}\sum_{\tau=1}^{v}\left(\overline{\omega}_{\ell\tau}\left(v_1(t)\right)\left(\underline{\eta}_{\ell\tau i_1 i_2\cdots i_z\kappa}^L-\overline{\eta}_{\ell\tau i_1 i_2\cdots i_z\kappa}^L\right)\right.\\&\left.\times e_1^{\mathrm{T}}(t)\left(\mathbf{Q}^L\mathbf{A}_\ell^{\mathrm{T}}+\mathbf{A}_\ell\mathbf{Q}^L+\mathbf{G}_\tau^{\mathrm{T}}\mathbf{B}_\ell^{\mathrm{T}}+\mathbf{B}_\ell\mathbf{G}_\tau-\mathbf{H}_{\ell\tau}^L+\mathbf{S}^L\right)e_1(t)\right)\end{aligned}\tag{28}$$

It is obvious that the negative definiteness of (28) can be achieved if the stability conditions (16)–(18) are satisfied by Theorem 1. This implies that the asymptotic stability of the error dynamics for Leader 1 is ensured based on the relationship in (27). In conclusion, the states of Leader 1 in the UNMAS are capable of tracking the desired state trajectory. □

By Theorem 1, the IT-2 fuzzy controller (6) can be designed for Leader 1. It is worth noting that the designed fuzzy controller can be directly extended to all other leaders in view of the homogeneity. In other words, the design approach of Theorem 1 enables the leaders to complete the formation task merely by properly assigning different target trajectories to each leader. However, the leaders are still required to provide a collision avoidance capability to lead the entire UNMAS away from potential dangers. Therefore, a collision avoidance algorithm combining the APF method with fuzzy theory is presented as follows.

Theorem 2: *Based on the IT-2 fuzzy FC designed in Theorem 1, the controller (6) is formulated as follows to simultaneously achieve the trajectory tracking and collision avoidance objectives.*

$$u_\alpha(t)=\sum_{\tau=1}^{v}\tilde{\Psi}_\tau\left(v_\alpha(t)\right)\left\{\mathbf{F}_\tau\left(x_\alpha(t)-\tilde{x}_\alpha^d(t)\right)\right\}\ \text{ for } \alpha=1,2,\ldots,m\tag{29}$$

where the desired state trajectories $\tilde{x}_\alpha^d(t)$ are designed by Algorithm 1.

Algorithm 1: The APF-based avoidance algorithm for adjusting the target state trajectory

Step 1: Set the parameters, including the detecting range R_{det}, the safety range R_{safe}, the effective range of the vortex potential field R_v, the effective range of the source potential field R_s, and the intensities of the vortex and source flows, k_v and k_s.

Step 2: Check the number of collision events within the detecting range R_{det}. If no events fall within the detecting range, terminate the algorithm and return to tracking mode.

Step 3: If any collision event enters the detecting range R_{det}, switch to collision avoidance mode and proceed to the next step. If no collision event is detected, skip to Step 7.

Step 4: Obtain the x and y positions, $x_\sigma^c(t)$ and $y_\sigma^c(t)$, as well as the longitudinal and lateral velocities, $V_{x\sigma}^c(t)$ and $V_{x\sigma}^c(t)$ of each detected collision event. Calculate DCPA_σ and TCPA_σ according to (14) and (15) in Definition 4. Moreover, the combination of the APF method with fuzzy theory, using vortex and source potential fields defined in Definitions 2 and 3, is designed as follows.
Vortex APF: Calculate $v_{vx\sigma}$ and $v_{vy\sigma}$ with the given parameter k_v by (12). Then, the desired orientation can be calculated as follows.

$$\psi_{vc\sigma} = atan2\left(v_{vy\sigma}, v_{vx\sigma}\right) \tag{30}$$

where $atan2\left(v_x, v_y\right)$ is the two-argument form of arctangent function, which considers the signs of both arguments v_x and v_y to determine the correct angle quadrant. Consequently, the following desired x and y positions can also be calculated for the trajectory tracking objective.

$${}_v x_{\alpha 1\sigma}^d(t) = x_{\alpha 1}(t) + \mathrm{Lcos}\left(\psi_{vc\sigma}\right) \tag{31}$$

$${}_v x_{\alpha 2\sigma}^d(t) = x_{\alpha 2}(t) + \mathrm{Lsin}\left(\psi_{vc\sigma}\right) \tag{32}$$

where L is the parameter that defines the tracking distance along the desired heading direction.
Source APF: Calculate $v_{sr\sigma}$ with the given parameter k_s by (13). Then, the desired orientation can also be calculated as follows.

$$\psi_{sc\sigma} = atan2\left(v_{sy\sigma}, v_{sx\sigma}\right) \tag{33}$$

As same as the design concept for (31) and (32), the desired positions are obtained based on (33) as follows.

$${}_s x_{\alpha 1\sigma}^d(t) = x_{\alpha 1}(t) + \mathrm{Lcos}\left(\psi_{sc\sigma}\right) \tag{34}$$

$${}_s x_{\alpha 2\sigma}^d(t) = x_{\alpha 2}(t) + \mathrm{Lsin}\left(\psi_{sc\sigma}\right) \tag{35}$$

According to the desired positions given in (31), (32), (34) and (35), the fuzzy logic is applied to achieve smoother switching between different APF modes. Thus, the final desired x and y positions for collision avoidance mode with the combined application of two APFs are derived as follows.

$$x_{\alpha 1\sigma}^{dc}(t) = \sum_{g=1}^{2} \phi_g^1(R_\sigma)\left\{{}_g x_{\alpha 1\sigma}^d(t)\right\} \tag{36}$$

$$x_{\alpha 2\sigma}^{dc}(t) = \sum_{g=1}^{2} \phi_g^1(R_\sigma)\left\{{}_g x_{\alpha 2\sigma}^d(t)\right\} \tag{37}$$

(Continued)

Algorithm 1 (continued)

where g with rule numbers 1 and 2 respectively denotes the positions derived from the vortex APF and source APF. The MF is designed as Fig. 1a below algorithm. Based on the positions in (36) and (37), the corresponding desired orientation is calculated as follows.

$$\psi_{\alpha\sigma}^{c} = atan2\left(x_{\alpha 2\sigma}^{dc}(t), {}_{c}x_{\alpha 1\sigma}^{dc}(t)\right) \tag{38}$$

Then, check whether $\mathrm{DCPA}_{\sigma} \le R_{safe}$ and $\mathrm{TCPA}_{\sigma} > 0$ for all σ. If the conditions are satisfied for at least one σ, proceed to the next step; if none of the events satisfies the conditions, skip to Step 6.

Step 5: If only one collision event satisfies the conditions, the final desired state trajectory $\tilde{x}_{\alpha}^{d}(t)$ for each leader is directly applied based on $x_{\alpha 1\sigma}^{dc}(t)$, $x_{\alpha 2\sigma}^{dc}(t)$ and $\psi_{\alpha\sigma}^{c}$ in (36)–(38). Note that the orientation in vehicle dynamics is commonly regarded as the third state. Therefore, $x_{\alpha 3\sigma}^{dc}(t) = \psi_{\alpha\sigma}^{c}$ is defined accordingly. Based on the setting, the desired trajectories for the IT-2 fuzzy FC (29) of leaders can be obtained by the following structure, where $\sigma = 1$ for only one collision event.

$$\tilde{x}_{\alpha}^{d}(t) = \left[x_{\alpha 11}^{dc}(t) \quad x_{\alpha 21}^{dc}(t) \quad x_{\alpha 31}^{dc}(t) \quad x_{\alpha 4}(t) \quad x_{\alpha 5}(t) \quad x_{\alpha 6}(t)\right]^{\mathrm{T}} \tag{39}$$

If more than one event satisfies the conditions, the elements of the final desired state trajectory vector $\tilde{x}_{\alpha}^{d}(t)$ are derived based on the TCPA factor as follows.

$$\tilde{x}_{\alpha 1}^{dca}(t) = \sum_{\sigma=1}^{\varsigma}\left(\frac{i\mathrm{TCPA}_{\sigma}}{i\mathrm{TCPA}_{total}}\right)\cdot x_{\alpha 1\sigma}^{dc}(t) \tag{40}$$

$$\tilde{x}_{\alpha 2}^{dca}(t) = \sum_{\sigma=1}^{\varsigma}\left(\frac{i\mathrm{TCPA}_{\sigma}}{i\mathrm{TCPA}_{total}}\right)\cdot x_{\alpha 2\sigma}^{dc}(t) \tag{41}$$

$$\tilde{x}_{\alpha 3}^{dca}(t) = atan2\left(\tilde{x}_{\alpha 2}^{dca}(t) - x_{\alpha 2}(t), \tilde{x}_{\alpha 1}^{dca}(t) - x_{\alpha 1}(t)\right) \tag{42}$$

where $i\mathrm{TCPA}_{\sigma} = \frac{1}{\mathrm{TCPA}_{\sigma}}$, $i\mathrm{TCPA}_{total} = i\mathrm{TCPA}_{1} + i\mathrm{TCPA}_{2} + \cdots i\mathrm{TCPA}_{\varsigma}$, and the index ς denotes the number of triggered collision events.

Then, the elements $\tilde{x}_{\alpha 1}^{d}(t)$, $\tilde{x}_{\alpha 2}^{d}(t)$ and $\tilde{x}_{\alpha 3}^{d}(t)$ in (40)–(42) are utilized in the design of the IT-2 fuzzy FC (29) for the collision avoidance scenarios.

$$\tilde{x}_{\alpha}^{d}(t) = \left[\tilde{x}_{\alpha 1}^{dca}(t) \quad \tilde{x}_{\alpha 2}^{dca}(t) \quad \tilde{x}_{\alpha 3}^{dca}(t) \quad x_{\alpha 4}(t) \quad x_{\alpha 5}(t) \quad x_{\alpha 6}(t)\right]^{\mathrm{T}} \tag{43}$$

Return to Step 2.

Step 6: Calculate the desired positions and orientation according to the results of (36) and (37) using the following procedure.

$${}_{ct}x_{\alpha 1\sigma}^{d}(t) = \sum_{g=1}^{2}\phi_{g}^{2}\left(DCPA_{\sigma}\right)\left\{{}_{g}x_{\alpha 1\sigma}^{dc}(t)\right\} \tag{44}$$

$${}_{ct}x_{\alpha 2\sigma}^{d}(t) = \sum_{g=1}^{2}\phi_{g}^{2}\left(DCPA_{\sigma}\right)\left\{{}_{g}x_{\alpha 2\sigma}^{dc}(t)\right\} \tag{45}$$

where g with rule numbers 1 and 2 respectively denotes the tracking mode and collision mode in this step, ${}_{1}x_{\alpha 1\sigma}^{dc}(t)$ and ${}_{1}x_{\alpha 2\sigma}^{dc}(t)$ represent the desired position trajectories in tracking mode assigned by the designer, ${}_{2}x_{\alpha 1\sigma}^{dc}(t)$ and ${}_{2}x_{\alpha 2\sigma}^{dc}(t)$ represent the desired position trajectories in collision mode calculated using (36) and (37), and the corresponding MF is designed as Fig. 1b.

(Continued)

Algorithm 1 (continued)

Then, the final desired trajectories of position and orientation are calculated based on the TCPA factor as follows.

$$\tilde{x}_{\alpha 1}^{dct}(t) = \sum_{\sigma=1}^{\varsigma} \left(\frac{i\mathrm{TCPA}_{\sigma}}{i\mathrm{TCPA}_{total}} \right) \cdot {}_{ct}x_{\alpha 1\sigma}^{d}(t) \tag{46}$$

$$\tilde{x}_{\alpha 2}^{dct}(t) = \sum_{\sigma=1}^{\varsigma} \left(\frac{i\mathrm{TCPA}_{\sigma}}{i\mathrm{TCPA}_{total}} \right) \cdot {}_{ct}x_{\alpha 2\sigma}^{d}(t) \tag{47}$$

$$\tilde{x}_{\alpha 3}^{dct}(t) = atan2\left(\tilde{x}_{\alpha 2}^{dct}(t) - x_{\alpha 2}(t), \tilde{x}_{\alpha 1}^{dct}(t) - x_{\alpha 1}(t) \right) \tag{48}$$

Using the elements (46)–(48), the vector $\tilde{x}_{\alpha}^{d}(t)$ of the desired state trajectory is constructed for the application of the IT-2 fuzzy FC (29) as follows.

$$\tilde{x}_{\alpha}^{d}(t) = \left[\tilde{x}_{\alpha 1}^{dct}(t) \quad \tilde{x}_{\alpha 2}^{dct}(t) \quad \tilde{x}_{\alpha 3}^{dct}(t) \quad x_{\alpha 4}(t) \quad x_{\alpha 5}(t) \quad x_{\alpha 6}(t) \right]^{\mathrm{T}} \tag{49}$$

Return to Step 2.

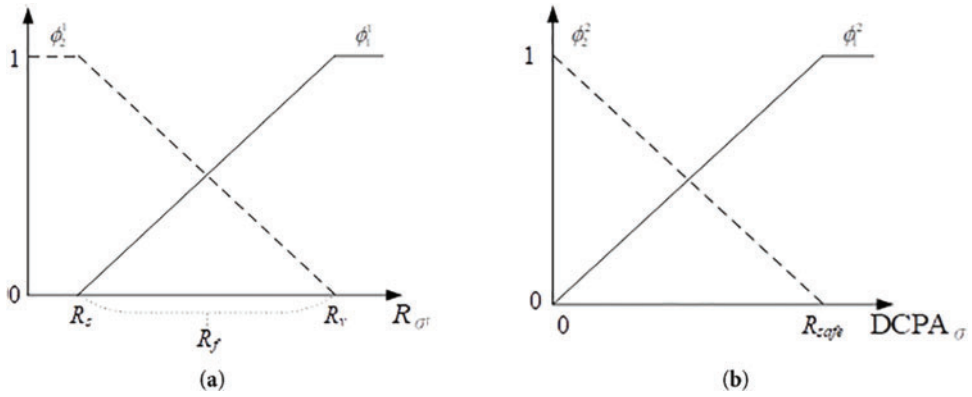

Figure 1: (**a**) MF associated with different APF strategies; (**b**) MF associated with different control modes

In Algorithm 1, the conditions $\mathrm{DCPA}_{\sigma} \leq R_{safe}$ and $\mathrm{TCPA}_{\sigma} > 0$ for determining whether the agents should switch to the full collision avoidance mode in Step 4 are adopted from [43]. Moreover, the TCPA factor is utilized to evaluate and integrate the target trajectories associated with multiple simultaneously triggered collision events. As shown in (40), (41), (46) and (47), the final target trajectory in collision mode is computed using a weighted average approach, where the inverse of each TCPA value is used as the weighting factor. This is because a smaller TCPA indicates a more imminent collision risk. Consequently, events with smaller TCPA values are assigned higher weights, allowing the agent to prioritize avoidance of more dangerous obstacles. It is worth noting that, in Step 4, fuzzy logic is employed to replace the direct switching between different orientations generated by distinct APFs. This is because the desired directions calculated by the vortex and source APFs are significantly different, and fuzzy logic can be applied to largely prevent abrupt switching.

The advantage of fuzzy logic lies in its ability to make the collision avoidance behavior of agents smoother and more reasonable. In Fig. 1a, the MF is designed to combine two different APFs using fuzzy logic. It is observed that when the distance to the potential collision event is less than R_v, the source APF gradually activates. As the distance decreases further, the influence of the source APF increases. Once the distance falls below R_s, the target trajectory is fully determined by the source APF to strongly prevent the agent from colliding with the obstacle.

Similar to this concept, the fuzzy logic is applied in Step 6 when at least one collision event is detected, but no condition triggers the avoidance conditions, which prevents abrupt switching between the tracking mode and collision avoidance mode. Based on Theorem 2 and Algorithm 1, an IT-2 fuzzy FC design approach with the collision avoidance capability is proposed for leaders to lead the entire UNMAS away from potential risks.

Then, based on the control command for the leaders given in (29), the IT-2 fuzzy CC design approach is presented in the following theorem.

Theorem 3. *If there exist the positive definite matrices* $\tilde{\mathbf{Q}}^F$, $\tilde{\mathbf{H}}^F_{\ell\tau}$, *the symmetric matrix* $\tilde{\mathbf{S}}^F$, *the matrices* $\tilde{\mathbf{N}}_\tau$, *and a minimized scalar* ρ *such that the following conditions are all satisfied based on the given scalars* $\overline{\eta}^F_{\ell\tau i_1 i_2 \cdots i_z \tilde{\kappa}}$, $\underline{\eta}^F_{\ell\tau i_1 i_2 \cdots i_z \tilde{\kappa}}$ *and* ξ, *the followers in the IT-2 T-SFM (10) can achieve the containment.*

$$\tilde{\mathbf{Q}}^F > 0 \text{ and } \tilde{\mathbf{H}}^F_{\ell\tau} > 0 \tag{50}$$

$$\begin{bmatrix} \tilde{\mathbf{A}}_\ell \tilde{\mathbf{Q}}^F + \tilde{\mathbf{Q}}^F \tilde{\mathbf{A}}_\ell^{\mathrm{T}} + \Xi_\beta \tilde{\mathbf{B}}_\ell \tilde{\mathbf{N}}_\tau + \tilde{\mathbf{N}}_\tau^{\mathrm{T}} \tilde{\mathbf{B}}_\ell^{\mathrm{T}} \Xi_\beta^{\mathrm{T}} + \xi \tilde{\mathbf{Q}}^F & * \\ -\tilde{\mathbf{B}}_\ell^{\mathrm{T}} & -\xi \mathbf{I}_h \end{bmatrix} - \tilde{\mathbf{H}}^F_{\ell\tau} + \tilde{\mathbf{S}}^F < 0$$

$$\text{for } \ell = 1, .., r \ \tau = 1, .., \nu \ \beta = 1, 2, 3, 4 \tag{51}$$

$$\sum_{\ell=1}^{r} \sum_{\tau=1}^{\nu} \left(\underline{\eta}_{\ell\tau i_1 i_2 \cdots i_z \kappa} \begin{bmatrix} \tilde{\mathbf{A}}_\ell \tilde{\mathbf{Q}}^F + \tilde{\mathbf{Q}}^F \tilde{\mathbf{A}}_\ell^{\mathrm{T}} + \Xi_\beta \tilde{\mathbf{B}}_\ell \tilde{\mathbf{N}}_\tau + \tilde{\mathbf{N}}_\tau^{\mathrm{T}} \tilde{\mathbf{B}}_\ell^{\mathrm{T}} \Xi_\beta^{\mathrm{T}} + \xi \tilde{\mathbf{Q}}^F & * \\ -\tilde{\mathbf{B}}_\ell^{\mathrm{T}} & -\xi \mathbf{I}_h \end{bmatrix} \right.$$
$$\left. - \left(\underline{\eta}_{\ell\tau i_1 i_2 \cdots i_z \kappa} - \overline{\eta}_{\ell\tau i_1 i_2 \cdots i_z \kappa} \right) \tilde{\mathbf{H}}^F_{\ell\tau} + \underline{\eta}_{\ell\tau i_1 i_2 \cdots i_z \kappa} \mathbf{S}^F \right) - \mathbf{S}^F < 0$$

$$\text{for } i_1, i_2 \cdots i_z = 1, 2 \tilde{\kappa} = 1, 2, \ldots, \delta^F \beta = 1, 2, 3, 4 \tag{52}$$

$$\begin{bmatrix} \tilde{\mathbf{Q}}^F & * \\ \tilde{\mathbf{Q}}^F & \rho^2 \mathbf{I}_s \end{bmatrix} \tag{53}$$

where $\tilde{\mathbf{N}}_\tau = \tilde{\mathbf{K}}_\tau \tilde{\mathbf{Q}}^F$, $\tilde{\mathbf{Q}}^F = \tilde{\mathbf{P}}_F^{-1}$, *the abbreviation* $\tilde{\mathbf{T}} = diag(\mathbf{T}, \mathbf{T})$ *stands for the matrices* $\mathbf{T} = \mathbf{A}_\ell, \mathbf{B}_\ell, \mathbf{N}_\tau, \mathbf{Q}^F, \mathbf{H}^F_{\ell\tau}, \mathbf{S}^F$, $diag(\cdot)$ *denotes the diagonal matrix with the elements* $\cdot$, $\Xi_\beta = \begin{bmatrix} Re\{\tilde{\lambda}_\beta\} & -Im\{\tilde{\lambda}_\beta\} \\ Im\{\tilde{\lambda}_\beta\} & Re\{\tilde{\lambda}_\beta\} \end{bmatrix}$, *the IT-2 MF-dependent parameters* $\overline{\eta}^F_{\ell\tau i_1 i_2 \cdots i_z \tilde{\kappa}}$ *and* $\underline{\eta}^F_{\ell\tau i_1 i_2 \cdots i_z \tilde{\kappa}}$ *are obtained with the same process in Theorem 1, and* $\tilde{\kappa}$ *is the division of sub-state space designed for the containment analysis.*

Proof of Theorem 3: To carry out the containment analysis, the containment error is first defined as follows for the IT-2 T-SFM (10).

$$e_F(t) = x_F(t) + \left(\mathbf{L}_1^{-1} \mathbf{L}_2 \otimes \mathbf{I}_s \right) x_L(t) \tag{54}$$

Based on the definition of the containment error in (54), the followers' dynamics can converge within the leaders' dynamics based on the properties of the Laplacian matrix in Lemma 2 if the error dynamics are stabilized. Then, the following derivative is obtained from (53).

$$\dot{e}_F(t) = \sum_{\ell=1}^{r} \sum_{\tau=1}^{\nu} \tilde{\Gamma}_{\ell\tau}(v_F(t)) \left\{ \left(\mathbf{I}_n \otimes \mathbf{A}_\ell + \mathbf{L}_1 \otimes \mathbf{B}_\ell \mathbf{K}_\tau \right) e_F(t) + \left(\mathbf{L}_1^{-1} \mathbf{L}_2 \otimes \mathbf{B}_\ell \right) u_L(t) \right\} \tag{55}$$

where $u_L(t) = \begin{bmatrix} u_1(t) & u_2(t) & \cdots & u_m(t) \end{bmatrix} \in \Re^{(h \times m)}$, $\tilde{\Gamma}_{\ell\tau}(v_F(t)) = \tilde{\Omega}_\ell(v_F(t)) \tilde{\Psi}_\tau(v_F(t))$. Therefore, the containment objective can be achieved by ensuring the convergence of the error dynamics in (54).

However, the control input of leaders $u_L(t)$ obtained from (29) also has an influence on the error dynamics system (55). Leveraging the IT-2 T-SFM representation, the analysis approach for linear MASs in [44] can be extended to solve the containment analysis problem as follows.

According to properties of Laplacian matrix in Lemma 1, the item associated with the vector $u_L(t)$ in (55) can be reconstructed by the following process.

$$u_{\alpha c}(t) = \sum_{\gamma=1}^{m} \varphi_{\alpha\gamma} u_\gamma(t) \; for \; \alpha = m+1, m+2, \ldots, m+n \tag{56}$$

where $\varphi_{\alpha\gamma}$ are the $(\alpha,\gamma)-th$ elements in the matrix $\mathbf{L}_1^{-1}\mathbf{L}_2$, which satisfy the following condition.

$$-\varphi_{\alpha\gamma} \geq 0 \text{ and } \sum_{\gamma=1}^{m} -\varphi_{\alpha\gamma} = 1 \tag{57}$$

Then, the upper bound condition can be derived for (56) using the inequality $2u_\gamma^{\mathrm{T}}(t)\,u_\wp(t) \leq u_\gamma^{\mathrm{T}}(t)\,u_\gamma(t) + u_\wp^{\mathrm{T}}(t)\,u_\wp(t)$.

$$\begin{aligned} u_{ac}^{\mathrm{T}}(t)\,u_{\alpha c}(t) &= \sum_{\gamma=1}^{m}\sum_{\wp=1}^{m} \varphi_{\alpha\gamma}\varphi_{\alpha\wp} u_\gamma^{\mathrm{T}}(t)\,u_\wp(t) \\ &\leq \frac{1}{2}\sum_{\gamma=1}^{m}\sum_{\wp=1}^{m} \varphi_{\alpha\gamma}\varphi_{\alpha\wp}\left(u_\gamma^{\mathrm{T}}(t)\,u_\gamma(t) + u_\wp^{\mathrm{T}}(t)\,u_\wp(t)\right) \leq \left(\sum_{\gamma=1}^{m}\varphi_{\alpha\gamma}\right)^2 \overline{u} \end{aligned} \tag{58}$$

Consequently, the fact $u_{ac}^{\mathrm{T}}(t)\,u_{\alpha c}(t) \leq \overline{u}$ can be derived due to the property of $\varphi_{\alpha\gamma}$. It is worth noting that an assumption regarding the existence of an upper bound on the control input of the leaders is given in [44], whereas the condition is not required in this research, as the tracking objective is fulfilled by the design of the IT-2 fuzzy FC (29). Based on the structure (56), the error dynamics system (55) is expressed into the following form.

$$\dot{e}_F(t) = \sum_{\ell=1}^{r}\sum_{\tau=1}^{v} \tilde{\Gamma}_{\ell\tau}(v_F(t))\left\{\left(\mathbf{I}_n \otimes \mathbf{A}_\ell + \mathbf{L}_1 \otimes \mathbf{B}_\ell\mathbf{K}_\tau\right) e_F(t) - \left(\mathbf{I}_n \otimes \mathbf{B}_\ell\right) u_{Lc}(t)\right\} \tag{59}$$

where $u_{Lc}(t) = \left[u_{(m+1)c}(t) \quad u_{(m+2)c}(t) \quad \cdots \quad u_{(m+3)c}(t)\right]^{\mathrm{T}}$, which satisfies the condition $\|u_{Lc}(t)\|^2 \leq n\overline{u}^2$ based on the relationship (58).

In order to reduce the conservativeness of the containment analysis using Lemma 2, the nonsingular matrix $\mathbf{W}$ is employed to derive the Jordan canonical form of (59).

$$\dot{\tilde{e}}_F(t) = \sum_{\ell=1}^{r}\sum_{\tau=1}^{v} \tilde{\Gamma}_{\ell\tau}(v_F(t))\left\{\left(\mathbf{I}_n \otimes \mathbf{A}_\ell + J_{\mathbf{L}_1} \otimes \mathbf{B}_\ell\mathbf{K}_\tau\right) \tilde{e}_F(t) - \left(\mathbf{I}_n \otimes \mathbf{B}_\ell\right) \tilde{u}_{Lc}(t)\right\} \tag{60}$$

where $\tilde{e}_F(t) = \left(\mathbf{W}^{-1} \otimes \mathbf{I}_s\right) e_F(t)$ and $\tilde{u}_{Lc}(t) = \left(\mathbf{W}^{-1} \otimes \mathbf{I}_s\right) u_{Lc}(t)$.

By expressing the variable in terms of the real part and the imaginary part, the error dynamic system (60) is reformulated in the following form.

$$\dot{\tilde{\tilde{e}}}_\alpha(t) = \sum_{\ell=1}^{r}\sum_{\tau=1}^{v} \tilde{\Gamma}_{\ell\tau}(v_\alpha(t))\left\{\left(\mathbf{A}_\ell + \Xi_\alpha\mathbf{B}_\ell\mathbf{K}_\tau\right) \tilde{\tilde{e}}_\alpha(t) - \mathbf{B}_\ell\tilde{\tilde{u}}_{\alpha c}(t)\right\} for \; \alpha = m+1, m+2, \ldots, m+n \tag{61}$$

where $\tilde{\tilde{e}}_\alpha(t) = \begin{bmatrix} Re\{\tilde{e}_\alpha(t)\} \\ Im\{\tilde{e}_\alpha(t)\} \end{bmatrix}$, $\tilde{\tilde{u}}_{\alpha c}(t) = \begin{bmatrix} Re\{\tilde{u}_{\alpha c}(t)\} \\ Im\{\tilde{u}_{\alpha c}(t)\} \end{bmatrix}$ and $\Xi_\alpha = \begin{bmatrix} Re\{\lambda_\alpha\} & -Im\{\lambda_\alpha\} \\ Im\{\lambda_\alpha\} & Re\{\lambda_\alpha\} \end{bmatrix}$.

Notably, the containment problem of system (59) with interaction among agents can be efficiently reduced to the analysis of individual follower agents by the expression of (61). To analysis the stability of dynamic system (61), the corresponding Lyapunov function is given as follows.

$$V_F\left(\tilde{\tilde{e}}_\alpha(t)\right) = \tilde{\tilde{e}}_\alpha^{\mathrm{T}}(t)\,\mathbf{P}_F\tilde{\tilde{e}}_\alpha(t) \tag{62}$$

where $\tilde{\mathbf{P}}_F = diag(\mathbf{P}_F, \mathbf{P}_F)$.

Following the analysis concept in [44], an ellipsoid is defined for the containment error dynamics.

$$E := \left\{\tilde{\tilde{e}}_\alpha(t) \,|\, \tilde{\tilde{e}}_\alpha^{\mathrm{T}}(t)\,\mathbf{P}_F\tilde{\tilde{e}}_\alpha(t) \le \overline{u}^2\right\} \tag{63}$$

Accordingly, the ellipsoid (63) can be ensured as an attractive invariant set if the following condition is satisfied.

$$\dot{V}_F\left(\tilde{\tilde{e}}_\alpha(t)\right) + \xi\left(V_F\left(\tilde{\tilde{e}}_\alpha(t)\right) - \tilde{\tilde{u}}_{\alpha c}^{\mathrm{T}}(t)\,\tilde{\tilde{u}}_{\alpha c}(t)\right) < 0 \tag{64}$$

Substituting (61), the following inequality can be obtained from (64).

$$\begin{aligned} &\sum_{\ell=1}^{r}\sum_{\tau=1}^{v}\tilde{\Gamma}_{\ell\tau}(\upsilon_\alpha(t)) \\ &\times\left\{\begin{bmatrix}\tilde{\tilde{e}}_\alpha(t)\\ \tilde{\tilde{u}}_{\alpha c}(t)\end{bmatrix}^{\mathrm{T}}\begin{bmatrix}\tilde{\mathbf{P}}_F\tilde{\mathbf{A}}_\ell + \tilde{\mathbf{P}}_F\tilde{\mathbf{A}}_\ell^{\mathrm{T}} + \tilde{\mathbf{P}}_F\Xi_\beta\tilde{\mathbf{B}}_\ell\tilde{\mathbf{K}}_\tau + \tilde{\mathbf{K}}_\tau^{\mathrm{T}}\tilde{\mathbf{B}}_\ell^{\mathrm{T}}\Xi_\beta^{\mathrm{T}}\tilde{\mathbf{P}}_F + \xi\tilde{\mathbf{P}}_F & * \\ -\tilde{\mathbf{B}}_\ell^{\mathrm{T}}\tilde{\mathbf{P}}_F & -\xi\mathbf{I}_h\end{bmatrix}\begin{bmatrix}\tilde{\tilde{e}}_\alpha(t)\\ \tilde{\tilde{u}}_{\alpha c}(t)\end{bmatrix}\right\} < 0 \end{aligned} \tag{65}$$

By following a similar analytical procedure as in (20)–(28), (65) is derived as the following inequality based on the IT-2 MF-dependent parameters.

$$\begin{aligned} &\begin{bmatrix}\tilde{\tilde{e}}_\alpha(t)\\ \tilde{\tilde{u}}_{\alpha c}(t)\end{bmatrix}^{\mathrm{T}}\left(\chi_{qi_q\tilde{\kappa}}\left(\upsilon_q^\alpha(t)\right)\sum_{\ell=1}^{r}\sum_{\tau=1}^{v}\left(\underline{\eta}^F_{\ell\tau i_1 i_2\cdots i_z\tilde{\kappa}}\begin{bmatrix}\tilde{\mathbf{A}}_\ell\tilde{\mathbf{Q}}^F + \tilde{\mathbf{Q}}^F\tilde{\mathbf{A}}_\ell^{\mathrm{T}} + \Xi_\alpha\tilde{\mathbf{B}}_\ell\tilde{\mathbf{N}}_\tau + \tilde{\mathbf{N}}_\tau^{\mathrm{T}}\tilde{\mathbf{B}}_\ell^{\mathrm{T}}\Xi_\alpha^{\mathrm{T}} + \xi\tilde{\mathbf{Q}}^F & * \\ -\tilde{\mathbf{B}}_\ell^{\mathrm{T}} & -\xi\mathbf{I}_h\end{bmatrix}\right.\right. \\ &\left.\left. -\left(\underline{\eta}^F_{\ell\tau i_1 i_2\cdots i_z\tilde{\kappa}} - \overline{\eta}^F_{\ell\tau i_1 i_2\cdots i_z\tilde{\kappa}}\right)\tilde{\mathbf{H}}^F_{\ell\tau} + \underline{\eta}^F_{\ell\tau i_1 i_2\cdots i_z\tilde{\kappa}}\tilde{\mathbf{S}}^F\right) - \tilde{\mathbf{S}}^F\right)\begin{bmatrix}\tilde{\tilde{e}}_\alpha(t)\\ \tilde{\tilde{u}}_{\alpha c}(t)\end{bmatrix} \\ &-\chi_{qi_q\tilde{\kappa}}\left(\upsilon_q^\alpha(t)\right)\sum_{\ell=1}^{r}\sum_{\tau=1}^{v}\left(\overline{\omega}_{\ell\tau}(\upsilon_\alpha(t))\left(\underline{\eta}^F_{\ell\tau i_1 i_2\cdots i_z\tilde{\kappa}} - \overline{\eta}^F_{\ell\tau i_1 i_2\cdots i_z\tilde{\kappa}}\right)\right. \\ &\times\left.\begin{bmatrix}\tilde{\tilde{e}}_\alpha(t)\\ \tilde{\tilde{u}}_{\alpha c}(t)\end{bmatrix}^{\mathrm{T}}\left(\begin{bmatrix}\tilde{\mathbf{A}}_\ell\tilde{\mathbf{Q}}^F + \tilde{\mathbf{Q}}^F\tilde{\mathbf{A}}_\ell^{\mathrm{T}} + \Xi_\alpha\tilde{\mathbf{B}}_\ell\tilde{\mathbf{N}}_\tau + \tilde{\mathbf{N}}_\tau^{\mathrm{T}}\tilde{\mathbf{B}}_\ell^{\mathrm{T}}\Xi_\alpha^{\mathrm{T}} + \xi\tilde{\mathbf{Q}}^F & * \\ -\tilde{\mathbf{B}}_\ell^{\mathrm{T}} & -\xi\mathbf{I}_h\end{bmatrix} - \tilde{\mathbf{H}}^F_{\ell\tau} + \tilde{\mathbf{S}}^F\right)\begin{bmatrix}\tilde{\tilde{e}}_\alpha(t)\\ \tilde{\tilde{u}}_{\alpha c}(t)\end{bmatrix}\right) < 0 \end{aligned} \tag{66}$$

It can be observed that inequality (66) is satisfied based on the relation (11) in Lemma 2 if the conditions (50)–(52) can be ensured by Theorem 3. Note that analyzing the stability of (60) is equivalent to analyzing the stability of (55).

After the ellipsoid is ensured as an attractive invariant set by satisfying (64), derived through (64)–(66), the minimization problem to ensure containment performance is solved as follows. From the condition (53)

in Theorem 3, the following relationship can be derived by multiplying $\tilde{\mathbf{P}}_F$ on both sides and applying the Schur complement.

$$\tilde{\tilde{e}}_\alpha^{\mathrm{T}}(t)\left(\rho^{-2}\mathbf{I}_q\right)\tilde{\tilde{e}}_\alpha(t) \leq \tilde{\tilde{e}}_\alpha^{\mathrm{T}}(t)\,\tilde{\mathbf{P}}_F\tilde{\tilde{e}}_\alpha(t) \leq \overline{u}^2 \tag{67}$$

The relationship (67) implies that $\left\|\tilde{\tilde{e}}_\alpha(t)\right\|^2 < \rho^2\overline{u}^2$. It is also deduced that the upper bound of the containment error energy can be minimized based on the definition in (62), the minimized parameter ρ, and the satisfaction of the condition (53) in Theorem 3. In conclusion, Problem 1 stated in [44] is solved such that the containment objective is achieved for the followers in the IT-2 T-SFM (10). It is worth noting that the IT-2 MF-dependent parameter division in the fuzzy CC design approach of Theorem 3 can be assigned different values from the fuzzy FC design approach of Theorem 1. □

By applying the IT-2 fuzzy F-and-C controller design approach from Theorems 1–3, the simulation of a multi-ship system is conducted in the next section to demonstrate the efficiency in formation, containment, and collision avoidance objectives.

4 Simulation of Multi-Ship System

In research [45,46], the authors developed a detailed method for mathematical modeling of ship steering using the kinematic and dynamic equations. Therefore, the following nonlinear multi-ship systems can be established by extending the results from [45–47].

$$\dot{x}_{\alpha1}(t) = cos\left(x_{\alpha3}(t)\right)x_{\alpha4}(t) - sin\left(x_{\alpha3}(t)\right)x_{\alpha5}(t) + \Delta_{\alpha1}(t)\,x_{\alpha4}(t) - \Delta_{\alpha2}(t)\,x_{\alpha5}(t) \tag{68}$$

$$\dot{x}_{\alpha2}(t) = sin\left(x_{\alpha3}(t)\right)x_{\alpha4}(t) + cos\left(x_{\alpha3}(t)\right)x_{\alpha5}(t) + \Delta_{\alpha2}(t)\,x_{\alpha4}(t) + \Delta_{\alpha1}(t)\,x_{\alpha5}(t) \tag{69}$$

$$\dot{x}_{\alpha3}(t) = x_{\alpha6}(t) + \Delta_\alpha(t)\,x_{\alpha6}(t) \tag{70}$$

$$\dot{x}_{\alpha4}(t) = -0.0318x_{\alpha4}(t) + 0.887u_{\alpha1}(t) \tag{71}$$

$$\dot{x}_{\alpha5}(t) = -0.0628x_{\alpha5}(t) - 0.003x_{\alpha6}(t) + 0.5415u_{\alpha2}(t) + 0.3152u_{\alpha3}(t) \tag{72}$$

$$\dot{x}_{\alpha6}(t) = -0.0045x_{\alpha5}(t) - 0.2427x_{\alpha6}(t) + 0.3152u_{\alpha2}(t) + 8.0082u_{\alpha3}(t) \tag{73}$$

where $x_{\alpha1}(t)$, $x_{\alpha2}(t)$ and $x_{\alpha3}(t)$ represent the x position, the y position and the yaw angle as described in the paragraph above Definition 2, $x_{\alpha4}(t)$, $x_{\alpha5}(t)$ and $x_{\alpha6}(t)$ represent the surge motion, sway motion and yaw angular velocity, $u_{\alpha1}(t)$, $u_{\alpha2}(t)$, $u_{\alpha3}(t)$ denote the forces and moment generated by the thrusters. To clarify the relationship between the system states in nonlinear multi-ship system (68)–(73) and the ship dynamics, the following diagram is provided with a single ship.

From Fig. 2, it can also be observed that the sway and surge motions differ from the velocities along the x and y axes. These velocities, used in the collision avoidance algorithm, can be calculated from the sway and surge motions based on the yaw angle. Specifically, the surge motion $x_{\alpha4}(t)$ and the sway motion $x_{\alpha5}(t)$ are required to be converted into longitudinal and lateral velocities prior to the application of the collision avoidance method in Theorem 2. Therefore, the following calculations are considered.

$$V_{\alpha x}(t) = x_{\alpha4}(t)\cos\left(x_{\alpha3}(t)\right) - x_{\alpha5}(t)\sin\left(x_{\alpha3}(t)\right) \tag{74}$$

$$V_{\alpha y}(t) = x_{\alpha4}(t)\sin\left(x_{\alpha3}(t)\right) + x_{\alpha5}(t)\cos\left(x_{\alpha3}(t)\right) \tag{75}$$

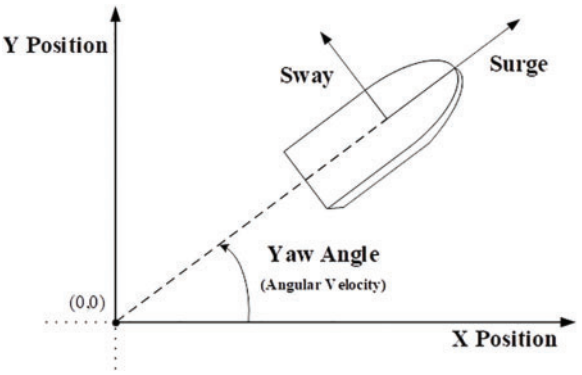

Figure 2: Diagram of a ship dynamic system

Considering the uncertain factors $\Delta_{\alpha 1}(t) = \cos(t)$ and $\Delta_{\alpha 2}(t) = \sin(t)$, the IT-2 T-SFM of the UNMAS (68)–(73) is constructed as follows.

$$\dot{x}_{\alpha}(t) = \sum_{\ell=1}^{r} \tilde{\Omega}_{\ell}(x_{\alpha 3}(t)) \{\mathbf{A}_{\ell} x_{\alpha}(t) + \mathbf{B}_{\ell} u_{\alpha}(t)\} \; for \; \alpha = 1, 2, \ldots, m+n \tag{76}$$

where

$x_{\alpha}(t) = \left[x_{\alpha 1}(t) \quad x_{\alpha 2}(t) \quad x_{\alpha 3}(t) \quad x_{\alpha 4}(t) \quad x_{\alpha 5}(t) \quad x_{\alpha 6}(t)\right]^{\mathrm{T}}$, $u_{\alpha}(t) = \left[u_{\alpha 1}(t) \quad u_{\alpha 2}(t) \quad u_{\alpha 3}(t)\right]^{\mathrm{T}}$, and the constant matrices are presented as follows.

$$\mathbf{A}_1 = \begin{bmatrix} 0 & 0 & 0 & cos(88^{\circ}) & -1 & 0 \\ 0 & 0 & 0 & 1 & cos(88^{\circ}) & 0 \\ 0 & 0 & 0 & 0 & 0 & 1 \\ 0 & 0 & 0 & -0.0318 & 0 & 0 \\ 0 & 0 & 0 & 0 & -0.0628 & -0.0030 \\ 0 & 0 & 0 & 0 & -0.0045 & -0.2427 \end{bmatrix},$$

$$\mathbf{A}_2 = \begin{bmatrix} 0 & 0 & 0 & 1 & -sin(2^{\circ}) & 0 \\ 0 & 0 & 0 & sin(2^{\circ}) & 1 & 0 \\ 0 & 0 & 0 & 0 & 0 & 1 \\ 0 & 0 & 0 & -0.0318 & 0 & 0 \\ 0 & 0 & 0 & 0 & -0.0628 & -0.0030 \\ 0 & 0 & 0 & 0 & -0.0045 & -0.2427 \end{bmatrix},$$

$$\mathbf{A}_3 = \begin{bmatrix} 0 & 0 & 0 & cos(-88^{\circ}) & 1 & 0 \\ 0 & 0 & 0 & -1 & cos(-88^{\circ}) & 0 \\ 0 & 0 & 0 & 0 & 0 & 1 \\ 0 & 0 & 0 & -0.0318 & 0 & 0 \\ 0 & 0 & 0 & 0 & -0.0628 & -0.0030 \\ 0 & 0 & 0 & 0 & -0.0045 & -0.2427 \end{bmatrix}, \text{ and } \mathbf{B}_{1\sim 3} = \begin{bmatrix} 0 & 0 & 0 \\ 0 & 0 & 0 \\ 0 & 0 & 0 \\ 0.8870 & 0 & 0 \\ 0 & 0.5415 & 0.3152 \\ 0 & 0.3152 & 8.0082 \end{bmatrix}.$$

It should be noted that the operating points for the linearization of subsystem in the IT-2 T-SFM (76) are chosen as $x_{\alpha 3}(t) = (90^{\circ}, 0^{\circ}, -90^{\circ})$. Based on these three operating points, the IT-2 MF for (76) is also designed in Fig. 3.

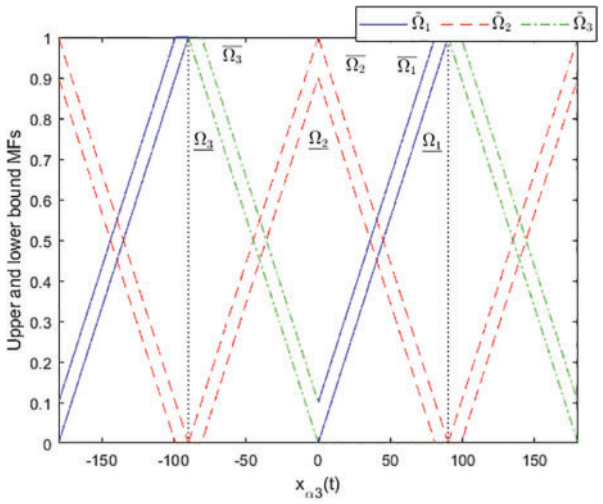

Figure 3: MF of nonlinear multi-ship system

Since the uncertain factors are considered with the value of 0.1 times of system parameters in the UNMAS (68)–(73), the range of interval in the IT-2 MF is also considered with 0.1 times of the original operating value. Since the uncertainties in the UNMAS (68)–(73) are considered as 10% of the system parameters, the interval width of the IT-2 MF is also set to 10% of the original operating range.

It is worth noting that the *x* position, *y* position, and yaw angle are selected as the tracking states in the trajectory tracking problem of this simulation. Therefore, the leader ships can reach the desired positions to complete the formation and maintain the correct course. However, the existing research on T-SFM modeling concerning the nonlinear ship system established in [45–47] has been primarily conducted within the yaw angle range of −90 to 90 degrees. These T-SFMs are not applicable and reasonable for yaw angle tracking. Therefore, the IT-2 MF originally defined over the range of −90 to 90 degrees is extended to cover a broader operating range, as illustrated in Fig. 3 so that all possible yaw angles in the x-y plane are included.

Based on the IT-2 T-SFM (76), the control problem verifying the formation, containment, and collision avoidance objectives is stated for the UNMASs (68)–(73) in Fig. 4.

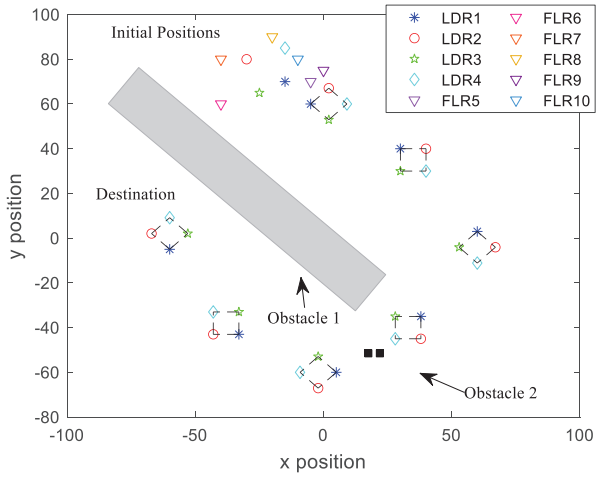

Figure 4: Control problem of multiple objectives

In the simulation of this research, "LDR" is used to denote leader ships numbered 1 to 4, and "FLR" is used to denote follower ships numbered 5 to 10. From the F-and-C control problem shown in Fig. 4, the initial and destination conditions are listed in the following Table 1. In addition, the position of Obstacle 2 is provided.

Table 1: Initial and destination conditions of all ships

Initial conditions				
LDR 1	**LDR 2**	**LDR 3**	**LDR 4**	**FLR 5**
$x_1(0) = \begin{bmatrix} -15 \\ 70 \\ 0 \\ 0 \\ 0 \\ 0 \end{bmatrix}$	$x_2(0) = \begin{bmatrix} -25 \\ 65 \\ 0 \\ 0 \\ 0 \\ 0 \end{bmatrix}$	$x_3(0) = \begin{bmatrix} -30 \\ 80 \\ 0 \\ 0 \\ 0 \\ 0 \end{bmatrix}$	$x_4(0) = \begin{bmatrix} -15 \\ 85 \\ 0 \\ 0 \\ 0 \\ 0 \end{bmatrix}$	$x_5(0) = \begin{bmatrix} -5 \\ 70 \\ 0 \\ 0 \\ 0 \\ 0 \end{bmatrix}$
FLR 6	**FLR 7**	**FLR 8**	**FLR 9**	**FLR 10**
$x_6(0) = \begin{bmatrix} -40 \\ 60 \\ 0 \\ 0 \\ 0 \\ 0 \end{bmatrix}$	$x_7(0) = \begin{bmatrix} -40 \\ 80 \\ 0 \\ 0 \\ 0 \\ 0 \end{bmatrix}$	$x_8(0) = \begin{bmatrix} -20 \\ 90 \\ 0 \\ 0 \\ 0 \\ 0 \end{bmatrix}$	$x_9(0) = \begin{bmatrix} 0 \\ 75 \\ 0 \\ 0 \\ 0 \\ 0 \end{bmatrix}$	$x_{10}(0) = \begin{bmatrix} -10 \\ 80 \\ 0 \\ 0 \\ 0 \\ 0 \end{bmatrix}$
Destinations				**Obstacles**
LDR 1	**LDR 2**	**LDR 3**	**LDR 4**	**2**
$x_1(0) = \begin{bmatrix} -60 \\ -5 \\ 0 \\ 0 \\ 0 \\ 0 \end{bmatrix}$	$x_1(0) = \begin{bmatrix} -67 \\ 2 \\ 0 \\ 0 \\ 0 \\ 0 \end{bmatrix}$	$x_1(0) = \begin{bmatrix} -53 \\ 2 \\ 0 \\ 0 \\ 0 \\ 0 \end{bmatrix}$	$x_1(0) = \begin{bmatrix} -60 \\ 9 \\ 0 \\ 0 \\ 0 \\ 0 \end{bmatrix}$	$\begin{bmatrix} 17.5 \\ -51.5 \\ 0 \\ 0 \\ 0 \\ 0 \end{bmatrix}, \begin{bmatrix} 22 \\ -51.5 \\ 0 \\ 0 \\ 0 \\ 0 \end{bmatrix}$

As shown in Fig. 4, the formation objective is to control the leader ships in maintaining a square formation until reaching the destination. Moreover, a known obstacle referred to as Obstacle 1 is located between the initial positions and the destination. The leader ships should bypass this obstacle through the design of the IT-2 fuzzy FC. In addition, unknown obstacles referred to as Obstacle 2 may emerge unpredictably in the ocean. The leader ships are expected to avoid both the unknown obstacles and collisions with other ships, including the followers, then return to the target trajectories. For the follower ships, the IT-2 fuzzy CC is designed to ensure that they remain within the square region formed by the leaders.

Based on the initial positions of all ships, the interaction topology is illustrated in Fig. 5, and the corresponding Laplacian matrix is constructed accordingly.

$$\mathbf{L}_1 = \begin{bmatrix} 3 & 0 & 0 & 0 & -1 & -1 \\ 0 & 2 & -1 & 0 & 0 & 0 \\ 0 & -1 & 3 & -1 & 0 & 0 \\ 0 & 0 & -1 & 3 & 0 & -1 \\ -1 & 0 & 0 & 0 & 2 & -1 \\ -1 & 0 & 0 & -1 & -1 & 3 \end{bmatrix} \text{and } \mathbf{L}_2 = \begin{bmatrix} -1 & 0 & 0 & 0 \\ 0 & 0 & -1 & 0 \\ 0 & -1 & 0 & 0 \\ 0 & 0 & 0 & -1 \\ 0 & 0 & 0 & 0 \\ 0 & 0 & 0 & 0 \end{bmatrix}. \tag{77}$$

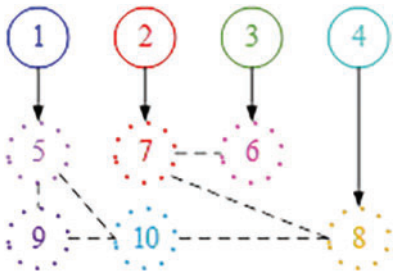

Figure 5: Interaction topology of multi-ship system

Thus, the elements in the adjacency matrix can be easily inferred from the Laplacian matrix (77). Subsequently, the IT-2 fuzzy formation-and-containment controller is designed based on the forms of (29) and (7) as follows.

$$u_\alpha(t) = \sum_{\tau=1}^{2} \tilde{\Psi}_\tau(v_\alpha(t)) \left\{ \mathbf{F}_\tau \left(x_\alpha(t) - \tilde{x}_\alpha^d(t) \right) \right\} for\ \alpha = 1,2,3,4 \tag{78}$$

$$u_\alpha(t) = \sum_{\tau=1}^{2} \tilde{\Psi}_\tau(v_\alpha(t)) \left\{ \mathbf{K}_\tau \sum_{\gamma \in N} a_{\alpha\gamma} \left(x_\alpha(t) - x_\gamma(t) \right) \right\} for\ \alpha = 5,6,\ldots,10 \tag{79}$$

where the IT-2 MF is designed in Fig. 6.

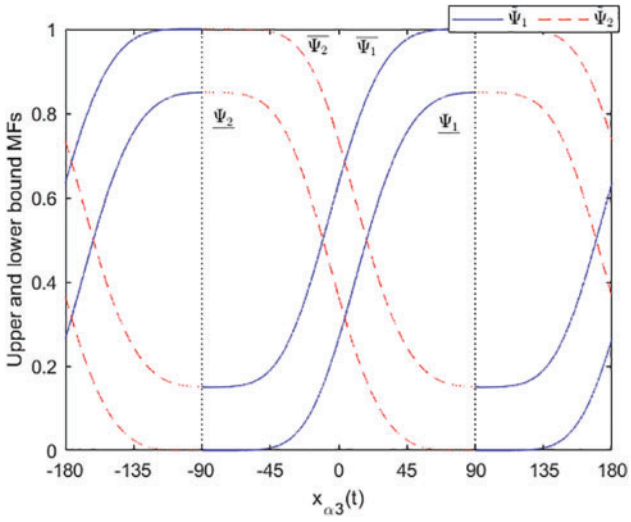

Figure 6: MF of IT-2 fuzzy F-and-C controller

It is worth noting that the number of rules and the shape of the IT-2 MF for the fuzzy controller can be designed independently from the IT-2 T-SFM (76) since the IPM concept. This flexibility allows the use of fewer fuzzy rules than required by the model, which effectively reduces the complexity and implementation cost of fuzzy controller. Without loss of generality, the IT-2 MF in Fig. 6 is also designed based on the operating points of 90 and −90 degrees. Moreover, the IT-2 MF designed between −90 and 90 degrees is further extended to a wider operating range to cover all the possible yaw angles.

Based on the IT-2 membership functions in Figs. 3 and 6, the following control gains are derived by solving the design problems stated in Theorems 1 and 3 using MATLAB, where the required parameters are set as $\delta^L = 20$ and $\delta^F = 30$.

$$\mathbf{F}_1 = \begin{bmatrix} -0.6013 & -0.4007 & -0.0101 & -2.4117 & -0.2879 & -0.0029 \\ 0.7777 & -0.6088 & 0.0346 & 0.5683 & -2.6147 & 0.0690 \\ -0.0311 & 0.0050 & -0.4411 & -0.0231 & 0.0359 & -0.8179 \end{bmatrix}$$

$$\mathbf{F}_2 = \begin{bmatrix} -0.6269 & 0.3987 & 0.0101 & -2.5153 & 0.2857 & 0.0029 \\ -0.7723 & -0.6624 & 0.0381 & -0.5650 & -2.8564 & 0.0770 \\ 0.0309 & 0.0077 & -0.4563 & 0.0229 & 0.0493 & -0.8580 \end{bmatrix} for\ \alpha = 1, 2, 3, 4 \tag{80}$$

$$\mathbf{K}_1 = 10^3 \times \begin{bmatrix} -1.0100 & -0.0393 & 0.0002 & -2.6319 & -0.1022 & 0.0002 \\ -0.0010 & -0.8399 & 0.0030 & -0.0020 & -2.1915 & 0.0032 \\ -0.0007 & 0.0307 & -0.0197 & -0.0019 & 0.0802 & -0.0237 \end{bmatrix}$$

$$\mathbf{K}_2 = 10^3 \times \begin{bmatrix} -0.9781 & 0.0164 & -0.0002 & -2.5488 & 0.0429 & -0.0001 \\ -0.0371 & -0.8140 & 0.0061 & -0.0955 & -2.1239 & 0.0070 \\ 0.0024 & 0.0287 & -0.0198 & 0.0062 & 0.0750 & -0.0238 \end{bmatrix} for\ \alpha = 5, 6, \ldots, 10 \tag{81}$$

After the control gains for the leader ships are determined, the following parameters are selected for the IT-2 fuzzy FC design in Theorem 2 and Algorithm 1 to achieve formation and collision avoidance simultaneously.

$$R_{det} = 3, R_{safe} = 3, R_v = 3, R_s = 1.5, R_f = 1, k_v = 1, k_s = 1, \mathrm{L} = 1. \tag{82}$$

By using MATLAB tools, including S-functions and Simulink, the simulation results and state response plots can be obtained as follows. Then, the following simulation results for the UNMASs (68)–(73) are obtained based on the conditions in Table 1 by applying the IT-2 fuzzy F-and-C controller (78), (79) with parameters (82).

From Figs. 7–9, it is evident that the state trajectories of leaders are effectively controlled to follow the target trajectories by the IT-2 fuzzy FC (78). That is, the x position and y position can achieve the assigned positions to complete the formation task. The desired yaw angle is also tracked to ensure the correctness of the ship course. Moreover, the state trajectories can also be adjusted to track the target trajectories computed by the collision avoidance algorithm. It is important to note that, regardless of whether in tracking or collision avoidance mode, the state trajectories of all followers remain within the leaders by the IT-2 fuzzy CC (79). Therefore, the followers can effectively avoid potential dangers by complying with the control commands of the leaders. In this research, the primary focus is on directly tracking the ships' positions and yaw angles. In other words, the surge motion, sway motion, and yaw angular velocity in Figs. 10–12 are automatically regulated by the ship to achieve this tracking objective. Nevertheless, the trajectories of these states for the followers can also be constrained within the interval defined by the leaders. To clearly present the simulation results, the ship trajectories corresponding to the control problem in Fig. 4 are shown in the following figure.

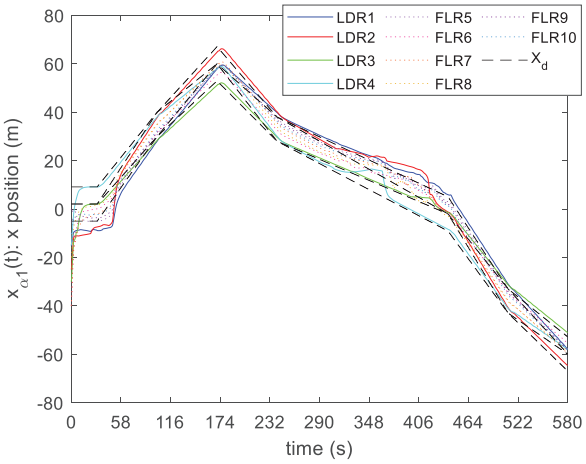

Figure 7: Responses of the x positions of all ships

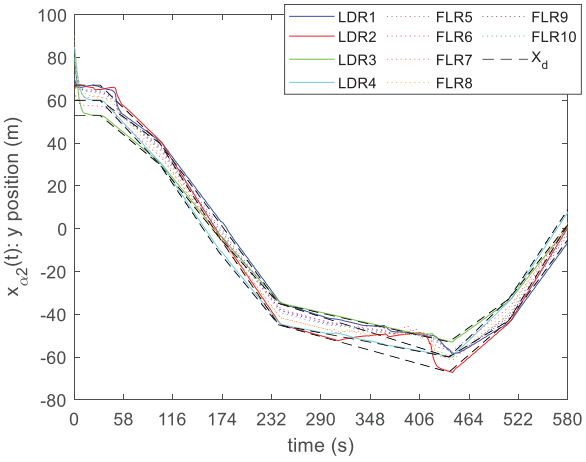

Figure 8: Responses of the y positions of all ships

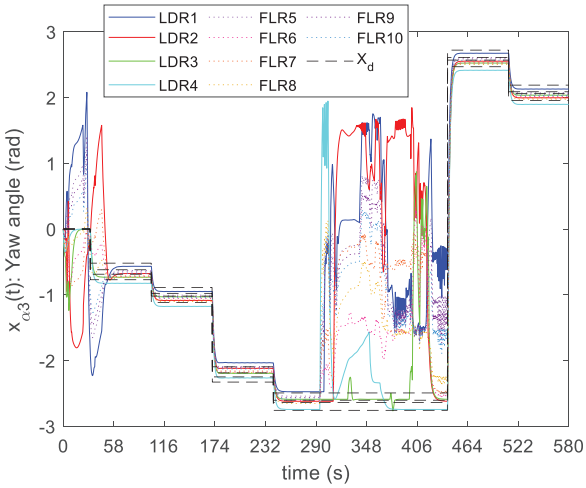

Figure 9: Responses of the yaw angles of all ships

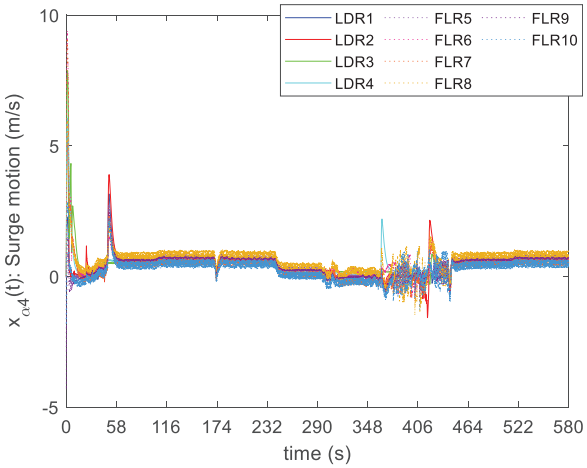

Figure 10: Responses of the surge motions of all ships

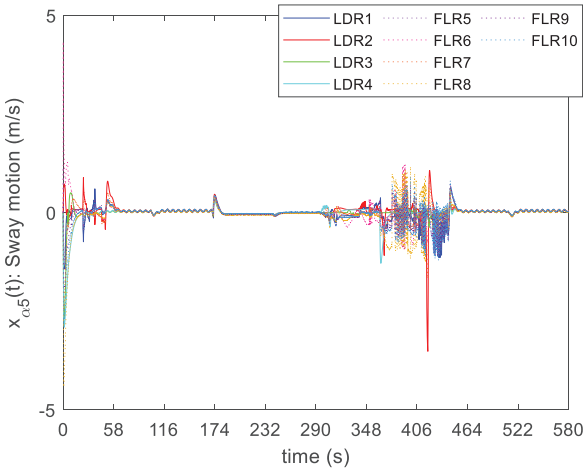

Figure 11: Responses of the sway motions of all ships

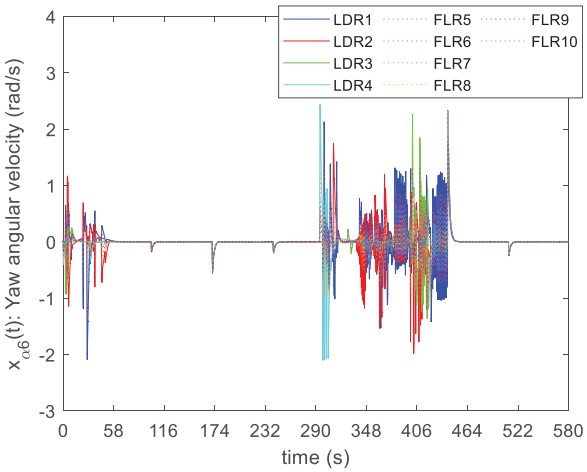

Figure 12: Responses of the yaw angular velocities of all ships

According to Fig. 13, it is demonstrated that the formation of the leaders and the dynamic behavior of this formation can be effectively achieved through the design of the IT-2 fuzzy FC (78) using the tracking technique individually. In addition, the leaders can bypass Obstacle 1 with just the proper design of the target trajectories and successfully arrive the destination. With the application of Algorithm 1, the leaders can also avoid collisions with other ships, including the followers, as shown in Fig. 14. It is worth noting that the followers are forced within the formation region defined by the leaders, using the IT-2 fuzzy CC (79), before the formation is fully completed.

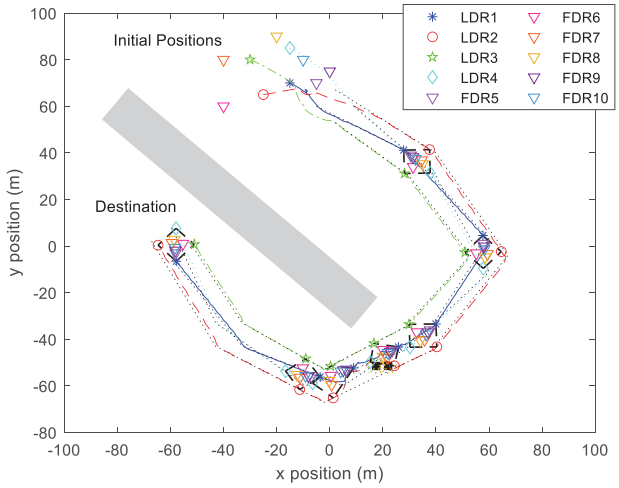

Figure 13: Trajectories of multi-ship system

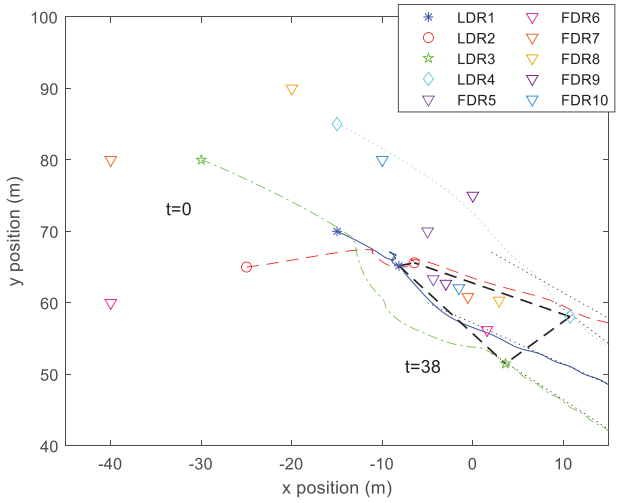

Figure 14: Zoomed-in view of initial trajectories

When the unpredictable Obstacle 2 occurs, the leaders can also adjust the positions and courses to effectively avoid the obstacle, which is seen in Fig. 15. In Fig. 15, the outer yellow dashed circle represents the effective range of the vortex APF, while the inner circle corresponds to the effective range of the source APF. It is observed that the leaders can guide the entire multi-ship system to successfully avoid collisions and subsequently return to the desired trajectory after the avoidance maneuver by the IT-2 fuzzy FC (78)

based on Algorithm 1. By the IT-2 fuzzy CC, the safety of all followers is ensured by maintaining within the formation throughout the entire period.

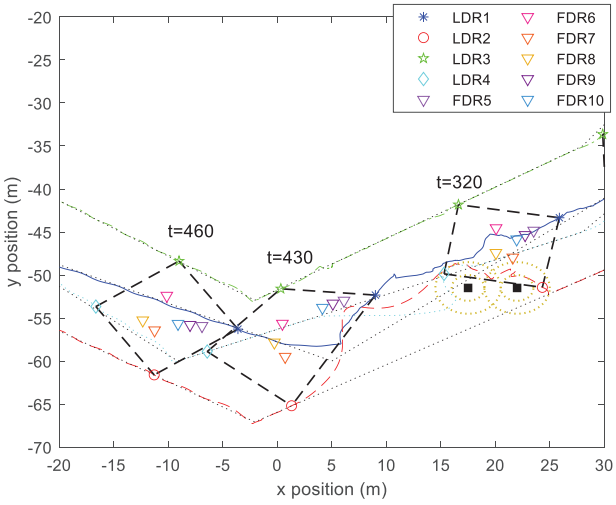

Figure 15: Zoomed-in view of trajectories during collision avoidance

From the simulation results in Figs. 7–9, it is observed that the tracking objective for all leaders is achieved at approximately 60 s. Moreover, the collision avoidance behavior is activated between 290 and 445 s. To verify the tracking error of the leaders, the periods before formation achievement and during collision avoidance should be excluded. Additionally, the most important states for the formation objective are the first two states, namely the x and y positions of the ships. Hence, the variance values of the tracking errors for all leaders are presented below to verify the effectiveness of the IT-2 fuzzy FC controller.

$$\begin{aligned}
&\text{LDR1: } var\left(x_{11}(t)-x_{11}^{d}(t)\right)=3.0257,\ var\left(x_{12}(t)-x_{12}^{d}(t)\right)=1.3114\\
&\text{LDR2: } var\left(x_{21}(t)-x_{21}^{d}(t)\right)=3.6954,\ var\left(x_{22}(t)-x_{22}^{d}(t)\right)=1.6736\\
&\text{LDR3: } var\left(x_{31}(t)-x_{31}^{d}(t)\right)=2.2511,\ var\left(x_{32}(t)-x_{32}^{d}(t)\right)=1.0792\\
&\text{LDR4: } var\left(x_{41}(t)-x_{41}^{d}(t)\right)=2.9580,\ var\left(x_{42}(t)-x_{42}^{d}(t)\right)=1.4152
\end{aligned} \tag{83}$$

where $var(\cdot)$ denotes the variance value of $\cdot$.

Based on the variance values presented in (83), it is observed that the tracking error variances for all leaders are within the units digit, which is relatively small compared to the overall range in the F-and-C problem of Fig. 4. These results verify the tracking accuracy under uncertainties using the proposed IT-2 fuzzy FC controller. For the followers in the multi-ship system, the containment objectives are demonstrated in Figs. 7–9 and Figs. 13–15. To further clarify the containment performance, the following results present the minimum and maximum distances from the followers to the convex hull, which is a square region formed by the leaders.

$$\begin{aligned}
&\text{FLR5: The maximum distance is 7.6390 and the minimum distance is 2.2468.}\\
&\text{FLR6: The maximum distance is 7.1273 and the minimum distance is 2.7593.}\\
&\text{FLR7: The maximum distance is 6.6618 and the minimum distance is 3.0773.}\\
&\text{FLR8: The maximum distance is 6.9046 and the minimum distance is 2.8289.}\\
&\text{FLR8: The maximum distance is 6.8898 and the minimum distance is 2.9968.}\\
&\text{FLR8: The maximum distance is 6.1400 and the minimum distance is 3.7474.}
\end{aligned} \tag{84}$$

From the simulation results in (84), it is verified that all the followers have remained within a certain distance from the convex hull formed by the leaders. This indicates that the followers are successfully contained within the square region. It can be concluded that a feasible and effective control method is provided by the IT-2 fuzzy F-and-C controller proposed in Theorems 1–3 of this research for the formation, containment and collision objectives.

Nevertheless, some visible fluctuations still occur in the collision avoidance scenarios shown in the above simulation results. These fluctuations are caused by abrupt switches between different APFs, as well as transitions between tracking and avoidance modes. To further reduce these fluctuations, effective methods such as the hybrid feedback proposed in [48] can be integrated into the collision avoidance algorithm to achieve smoother switching performance. Although this study validates the proposed IT-2 fuzzy F-and-C controller with collision avoidance on a multi-ship system, the approach is applicable to a wide range of NMASs, including unmanned aerial vehicles, ground vehicles, and surface vehicles. It should be noted that formation, containment, and collision avoidance are primarily considered in systems where the control of positions and trajectories is essential, such as unmanned vehicles. The fuzzy controller based on the IT-2 T-SFM also effectively solve the uncertainty problem, which are critical and unavoidable in these vehicles. Therefore, the proposed IT-2 fuzzy F-and-C controller design can be extended beyond maritime applications to enhance the cooperative control performance and safety of other unmanned vehicles. However, this research still establishes the first successful integration of the IT-2 fuzzy formation-and-containment controller design with a collision avoidance capability.

5 Conclusion

An IT-2 F-and-C design approach with collision avoidance capability is proposed in this research for UNMASs based on the combination of the APF method and fuzzy theory. First, the IT-2 T-SFM is adopted to provide a more comprehensive representation for UNMASs under uncertain factors. Based on the modeling process, the IT-2 T-SFM for the target trajectory is also constructed for the formation objective. Unlike the existing F-and-C works, the IT-2 fuzzy FC for the leaders is individually designed using a tracking control approach. This scheme simplifies the formation controller design process and reduces implementation complexity. Notably, since the tracking controller is originally designed to achieve the formation objective, it can also be naturally applied to track the desired trajectories generated by the APF method in the avoidance mode. Through the combined application of the source and vortex APFs, the leaders are repelled from the obstacle and guided to turn right to bypass the collision. In this research, fuzzy logic is applied to enable smoother adjustments between these two APFs and enhance the avoidance behavior. By extending the analysis methods for linear MASs, the analysis problem for the IT-2 fuzzy CC design approach can still be solved, even when the leaders' control inputs involve both tracking and avoidance modes. In other words, the containment objective can be maintained in both scenarios, which allows the followers to remain within the leaders' formation and avoid potential collisions. Finally, the simulation results of a multi-ship system are presented to verify the control performance of multiple objectives. According to the results, it is observed that the integration of the collision avoidance algorithm successfully turns the leaders' course to avoid potential dangers. Moreover, the followers can avoid collisions by adhering to the leaders' formation and trajectories. It can be proven that the safety of the entire multi-ship system is enhanced when the collision avoidance capability of the leaders is ensured. In conclusion, the proposed IT-2 fuzzy F-and-C controller design approach provides a feasible and effective control scheme for UNMASs to simultaneously accomplish formation, containment, and collision avoidance tasks. In this research, the leaders achieve the formation purpose without using communication. However, the containment purpose of followers heavily depends on the dynamics of other agents, which means that communication is unavoidable. Therefore, fault and

attack problems constitute promising directions for future work within the proposed design framework. Moreover, considering the practical application of multi-ship systems, issues such as measurement noise, communication delays, and environmental disturbances should also be discussed in future work.

Acknowledgement: Not applicable.

Funding Statement: This research was founded by the National Science and Technology Council of the Republic of China under contract NSTC113-2221-E-019-032.

Author Contributions: The authors confirm contribution to the paper as follows: Conceptualization, Yann-Horng Lin, Wen-Jer Chang and Yi-Chen Lee; methodology, Yann-Horng Lin, Yi-Chen Lee and Wen-Jer Chang; software, Yann-Horng Lin, Cheung-Chieh Ku and Muhammad Shamrooz Aslam; validation, Wen-Jer Chang, Muhammad Shamrooz Aslam and Cheung-Chieh Ku; formal analysis, Yi-Chen Lee and Muhammad Shamrooz Aslam; investigation, Yann-Horng Lin, Muhammad Shamrooz Aslam and Wen-Jer Chang; resources, Wen-Jer Chang, Yi-Chen Lee and Cheung-Chieh Ku; data curation, Yann-Horng Lin and Cheung-Chieh Ku; writing—original draft preparation, Yann-Horng Lin; writing—review and editing, Wen-Jer Chang, Yi-Chen Lee and Cheung-Chieh Ku; visualization, Yann-Horng Lin, Muhammad Shamrooz Aslam and Cheung-Chieh Ku; supervision, Wen-Jer Chang and Cheung-Chieh Ku; project administration, Wen-Jer Chang and Yi-Chen Lee; funding acquisition, Wen-Jer Chang. All authors reviewed the results and approved the final version of the manuscript.

Availability of Data and Materials: All data generated or analyzed during this study are included in this published article.

Ethics Approval: Not applicable.

Conflicts of Interest: The authors declare no conflicts of interest to report regarding the present study.

Abbreviations

IT-2	Interval Type-2
MAS	Multi-Agent System
NMAS	Nonlinear MAS
UNMAS	Uncertain NMAS
T-SFM	Takagi-Sugeno Fuzzy Model
FC	Formation Controller
CC	Containment Controller
F-and-C	Formation and Containment
IPM	Imperfect Premise Matching
APF	Artificial Potential Field
MF	Membership Function
LMI	Linear Matrix Inequality

References

1. Zhu Z, Du Q, Wang Z, Li G. A survey of multi-agent cross domain cooperative perception. Electronics. 2022;11(7):1091. doi:10.3390/electronics11071091.
2. Lizzio FF, Capello E, Guglieri G. A review of consensus-based multi-agent UAV implementations. J Intell Robot Syst. 2022;106(2):43. doi:10.1007/s10846-022-01743-9.
3. Kwon JW. Cooperative environment scans based on a multi-robot system. Sensors. 2015;15(3):6483–96. doi:10.3390/s150306483.
4. Li Z, Mazouchi M, Modares H, Wang X, Sun J. Finite-time adaptive output synchronization of uncertain nonlinear heterogeneous multi-agent systems. Int J Robust Nonlinear Control. 2021;31(18):9416–35. doi:10.1002/rnc.5779.

5. Tang L, Zhang L, Xu N. Optimized backstepping-based finite-time containment control for nonlinear multi-agent systems with prescribed performance. Optim Control Appl Methods. 2024;45(5):2364–82. doi:10.1002/oca.3160.
6. Shamrooz Aslam M, Bilal H, Chang WJ, Yahya A, Anjum Badruddin I, Kamangar S, et al. Formation control of heterogeneous multi-agent systems under fixed and switching hierarchies. IEEE Access. 2024;12:97868–82. doi:10.1109/access.2024.3419815.
7. Li D, Ge SS, Ma G, He W. Layered formation-containment control of multi-agent systems in constrained space. Int J Control Autom Syst. 2020;18(3):768–79. doi:10.1007/s12555-019-0172-8.
8. Zhou Y, Liu Y, Zhao Y, Wen G. Appointed-time formation-containment control for nonlinear multi-agent networks using sample-data feedback. Int J Robust Nonlinear Control. 2023;33(8):4616–35. doi:10.1002/rnc.6635.
9. Alsinai A, Ali Al-Shamiri MM, Ul Hassan W, Rehman S, Niazi AUK. Fuzzy adaptive approaches for robust containment control in nonlinear multi-agent systems under false data injection attacks. Fractal Fract. 2024;8(9):506. doi:10.3390/fractalfract8090506.
10. Wang Y, Zhong Y, Zhang Y, Shi Y, Chen H. Unmanned aerial vehicle formation control method based on improved artificial potential field and consensus. IET Control Theory Appl. 2024;18(18):2555–67. doi:10.1049/cth2.12772.
11. Tang C, Ji L, Yang S, Guo X, Li H. Prescribed-time containment control of multi-agent systems subject to collision avoidance and connectivity maintenance. ISA Trans. 2024;148:156–68. doi:10.1016/j.isatra.2024.03.002.
12. He Z, Liu C, Chu X, Negenborn RR, Wu Q. Dynamic anti-collision A-star algorithm for multi-ship encounter situations. Appl Ocean Res. 2022;118:102995. doi:10.1016/j.apor.2021.102995.
13. Pandav P, Ren J. A data-driven approach to motion planning and optimal control of medical nanorobots with dynamic window approach. IFAC-PapersOnLine. 2023;56(3):583–8. doi:10.1016/j.ifacol.2023.12.087.
14. Tang W, Zhou Y, Zhang T, Liu Y, Liu J, Ding Z. Cooperative collision avoidance in multirobot systems using fuzzy rules and velocity obstacles. Robotica. 2023;41(2):668–89. doi:10.1017/s0263574722001515.
15. Xi Z, Han H, Cheng J, Lv M. Reducing oscillations for obstacle avoidance in a dense environment using deep reinforcement learning and time-derivative of an artificial potential field. Drones. 2024;8(3):85. doi:10.3390/drones8030085.
16. Wang HO, Tanaka K, Griffin MF. An approach to fuzzy control of nonlinear systems: stability and design issues. IEEE Trans Fuzzy Syst. 1996;4(1):14–23. doi:10.1109/91.481841.
17. Chang CW, Tao CW. A novel approach to implement Takagi-sugeno fuzzy models. IEEE Trans Cybern. 2017;47(9):2353–61. doi:10.1109/TCYB.2017.2701900.
18. Su CL, Lee YC, Chang WJ, Ku CC. Decentralized optimal passive control for discrete-time Takagi-Sugeno interconnected descriptor systems with uncertainties. Int J Fuzzy Syst. 2024;26(4):1175–90. doi:10.1007/s40815-023-01659-y.
19. Lee YC, Lin YH, Chang WJ, Aslam MS, Lin ZY. Optimal fuzzy tracking synthesis for nonlinear discrete-time descriptor systems with T-S fuzzy modeling approach. Comput Model Eng Sci. 2025;143(2):1433–61. doi:10.32604/cmes.2025.064717.
20. Akka K, Khaber F. Optimal fuzzy tracking control with obstacles avoidance for a mobile robot based on Takagi-Sugeno fuzzy model. Trans Inst Meas Control. 2019;41(10):2772–81. doi:10.1177/0142331218811462.
21. Wang X, Ma H, Kang H. Fuzzy adaptive group obstacle avoidance control for second-order multi-agent systems under fixed and switching topologies. IEEE Trans Netw Sci Eng. 2023;10(2):619–30. doi:10.1109/TNSE.2022.3213342.
22. Ebrahimi A, Farrokhi M. Multi-agent flocking with obstacle avoidance and safety distance preservation: a fuzzy potential-based approach. Intell Serv Robot. 2024;17(2):181–95. doi:10.1007/s11370-023-00500-7.
23. Tsai CC, Wu HL, Tai FC, Chen YS. Distributed consensus formation control with collision and obstacle avoidance for uncertain networked omnidirectional multi-robot systems using fuzzy wavelet neural networks. Int J Fuzzy Syst. 2017;19(5):1375–91. doi:10.1007/s40815-016-0239-0.
24. Chang Z, Zong G, Song S, Zhao X. Fast finite-time bipartite formation with obstacle avoidance for time-delay multiagent systems: application in mobile robot swarm. IEEE Trans Ind Inform. 2025;21(6):4586–94. doi:10.1109/TII.2025.3545050.

25. Keshavarz-Ghorabaee M. Sustainable supplier selection and order allocation using an integrated ROG-based type-2 fuzzy decision-making approach. Mathematics. 2023;11(9):2014. doi:10.3390/math11092014.
26. Men J, Zhao C. A Type-2 fuzzy hybrid preference optimization methodology for electric vehicle charging station location. Energy. 2024;293:130701. doi:10.1016/j.energy.2024.130701.
27. Mendel JM. Type-2 fuzzy sets and systems: an overview. IEEE Comput Intell Mag. 2007;2(1):20–9. doi:10.1109/MCI.2007.380672.
28. Karnik NN, Mendel JM. Operations on type-2 fuzzy sets. Fuzzy Sets Syst. 2001;122(2):327–48. doi:10.1016/S0165-0114(00)00079-8.
29. Mendel JM, John RI, Liu F. Interval type-2 fuzzy logic systems made simple. IEEE Trans Fuzzy Syst. 2006;14(6):808–21. doi:10.1109/TFUZZ.2006.879986.
30. Wang JC, Wang FH, He R, Lv LF. Anti-lock braking control using an interval type-2 fuzzy neural network scheme for electric vehicles. Proc Inst Mech Eng Part D J Automob Eng. 2024;238(14):4534–50. doi:10.1177/09544070231197856.
31. Al-Mallah M, Ali M, Al-Khawaldeh M. Obstacles avoidance for mobile robot using type-2 fuzzy logic controller. Robotics. 2022;11(6):130. doi:10.3390/robotics11060130.
32. Lin YH, Chang WJ, Ku CC. Solving the formation and containment control problem of nonlinear multi-boiler systems based on interval type-2 Takagi-Sugeno fuzzy models. Processes. 2022;10(6):1216. doi:10.3390/pr10061216.
33. Afaghi A, Ghaemi S, Ghiasi AR, Ali Badamchizadeh M. Type-2 fuzzy consensus control of nonlinear multi-agent systems: an LMI approach. J Frankl Inst. 2021;358(8):4326–47. doi:10.1016/j.jfranklin.2021.03.024.
34. Hua M, Ding H, Yao XY, Zhang X. Distributed fixed-time formation-containment control for multiple Euler-Lagrange systems with directed graphs. Int J Control Autom Syst. 2021;19(2):837–49. doi:10.1007/s12555-020-0106-5.
35. Li C, Chen L, Guo Y, Ma G. Formation-containment control for networked Euler-Lagrange systems with input saturation. Nonlinear Dyn. 2018;91(2):1307–20. doi:10.1007/s11071-017-3946-7.
36. Lam HK, Li H, Deters C, Secco EL, Wurdemann HA, Althoefer K. Control design for interval type-2 fuzzy systems under imperfect premise matching. IEEE Trans Ind Electron. 2014;61(2):956–68. doi:10.1109/TIE.2013.2253064.
37. Zhang Z, Dong J. Containment control of interval type-2 fuzzy multi-agent systems with multiple intermittent packet dropouts and actuator failure. J Frankl Inst. 2020;357(10):6096–120. doi:10.1016/j.jfranklin.2020.04.003.
38. Chang WJ, Lin YH, Ku CC. Passive formation and containment control of multiple nonlinear autonomous ship systems with external disturbances based on interval type-2T-S fuzzy model. Int J Fuzzy Syst. 2024;26(8):2505–17. doi:10.1007/s40815-024-01742-y.
39. Chang WJ, Lin YH, Lee YC, Ku CC. Investigating formation and containment problem for nonlinear multiagent systems by interval type-2 fuzzy sliding mode tracking approach. IEEE Trans Fuzzy Syst. 2024;32(7):4163–77. doi:10.1109/tfuzz.2024.3387045.
40. Tanakitkorn K. Fuzzy-based potential field collision avoidance technique for unmanned surface vehicles. IOP Conf Ser Mater Sci Eng. 2021;1137(1):012017. doi:10.1088/1757-899x/1137/1/012017.
41. Xi J, Shi Z, Zhong Y. Consensus analysis and design for high-order linear swarm systems with time-varying delays. Phys A Stat Mech Its Appl. 2011;390(23–24):4114–23. doi:10.1016/j.physa.2011.06.045.
42. Shibata N, Sugiyama S, Wada T. Collision avoidance control with steering using velocity potential field. In: 2014 IEEE Intelligent Vehicles Symposium Proceedings; 2014 Jun 8–11; Dearborn, MI, USA. p. 438–43. doi:10.1109/IVS.2014.6856469.
43. Lee MC, Nieh CY, Kuo HC, Huang JC. A collision avoidance method for multi-ship encounter situations. J Mar Sci Technol. 2020;25(3):925–42. doi:10.1007/s00773-019-00691-8.
44. Li P, Jabbari F, Sun XM. Containment control of multi-agent systems with input saturation and unknown leader inputs. Automatica. 2021;130:109677. doi:10.1016/j.automatica.2021.109677.
45. Fossen TI. Guidance and control of ocean vehicles. Chichester, UK: John Wiley & Sons; 1994.
46. Fossen TI, Grovlen A. Nonlinear output feedback control of dynamically positioned ships using vectorial observer backstepping. IEEE Trans Control Syst Technol. 1998;6(1):121–8. doi:10.1109/87.654882.

47. Lin YH, Chang WJ, Pen CL. Fuzzy steering control for TS fuzzy model-based multiple ship systems subject to formation and containment. Int J Fuzzy Syst. 2023;25(5):1782–94. doi:10.1007/s40815-023-01479-0.
48. Berkane S, Bisoffi A, Dimarogonas DV. Obstacle avoidance via hybrid feedback. IEEE Trans Autom Control. 2021;67(1):512–9. doi:10.1109/TAC.2021.3086329.